Article

Current Biology

Integrative phenotyping reveals new insights into the anemonefish adaptive radiation

Highlights

- Anemonefish diversification is shaped by multiple factors beyond host specificity
- Distinct eco-morphotypes differ in morphology, behavior, and swimming ability
- Integrating field, lab, and modeling deepens understanding of diversification
- Functional studies highlight the ecological significance of phenotypic traits

Authors

Manon Mercader, Fabienne Ziadi-Künzli, Stefano Olivieri, Shinya Komoto, Marco Edoardo Rosti, Bruno Frédérich, Vincent Laudet

Correspondence

manon.mercader@oist.jp (M.M.), vincent.laudet@oist.jp (V.L.)

In brief

Mercader et al. investigate anemonefish diversification using an interdisciplinary approach combining fieldwork, lab experiments, and modeling. Focusing on swimming abilities, behavior, and morphology, they identify eco-morphotypes, showing that diversification involves multiple ecological strategies beyond host use.

Mercader et al., 2025, Current Biology *35*, 3473–3487
July 21, 2025
https://doi.org/10.1016/j.cub.2025.06.041

CellPress

Current Biology

CellPress

Article

Integrative phenotyping reveals new insights into the anemonefish adaptive radiation

Manon Mercader,[1,10,*] Fabienne Ziadi-Künzli,[2] Stefano Olivieri,[3,4,5] Shinya Komoto,[6] Marco Edoardo Rosti,[2] Bruno Frédérich,[7] and Vincent Laudet[1,8,9,*]

[1]Marine Eco-Evo-Devo Unit, Okinawa Institute of Science and Technology Graduate University, Onna-son, Okinawa 904-0495, Japan
[2]Nonlinear and Non-equilibrium Physics Unit, Okinawa Institute of Science and Technology Graduate University, Onna-son, Okinawa 904-0495, Japan
[3]Complex Fluids and Flows Unit, Okinawa Institute of Science and Technology Graduate University, Onna-son, Okinawa 904-0495, Japan
[4]Department of Civil, Chemical, and Environmental Engineering, University of Genova, 16126 Genova, Italy
[5]Istituto Nazionale di Fisica Nucleare, Sezione di Genova, 16146 Genova, Italy
[6]Scientific Imaging Section, Okinawa Institute of Science and Technology Graduate University, Onna-son, Okinawa 904-0495, Japan
[7]Laboratory of Evolutionary Ecology, FOCUS, University of Liège, 4000 Liège, Belgium
[8]Marine Research Station, Institute of Cellular and Organismic Biology, Academia Sinica, Jiaoxi, Yilan 262, Taiwan
[9]CNRS IRL 2028 "Eco-Evo-Devo of Coral Reef Fish Life Cycle" (EARLY), Onna-son, Okinawa 904-0495, Japan
[10]Lead contact
*Correspondence: manon.mercader@oist.jp (M.M.), vincent.laudet@oist.jp (V.L.)
https://doi.org/10.1016/j.cub.2025.06.041

SUMMARY

Evolutionary radiations are fundamental to the generation of biodiversity, occurring when organisms rapidly diversify to exploit various ecological niches. Symbiosis can serve as a powerful catalyst for such diversification, as illustrated by the iconic association of anemonefish and sea anemones. However, a critical gap in our understanding of adaptive radiations lies in determining how ecological opportunities drive adaptive morphological, behavioral, and physiological traits and how these traits, in turn, influence diversification. Using anemonefish (*Amphiprion* spp.) as a model, we investigated the phenotypic diversification accompanying their evolutionary history following symbiosis with giant sea anemones. While host specificity has traditionally been viewed as the primary driver of anemonefish adaptive radiation, we present an alternative perspective, showing that distinct ecological strategies—independent of host species—may also significantly contribute to their diversification. By examining half of the described anemonefish species, we combined field observations, swimming tunnel experiments, computational simulations, and morphological analyses to empirically reveal the presence of eco-morphotypes that exist independently of host specificity. Our findings provide novel insights into the evolutionary history and processes shaping anemonefish diversity. We show that, beyond sea anemone hosts, multiple drivers significantly contributed to their diversification. Integrative phenotyping, combining *in situ* and laboratory observations, reveals the forces driving adaptive radiations. It uncovers an unexpected, fine-tuned diversification in anemonefish, exemplifying how natural selection precisely shapes biodiversity during radiative bursts and highlighting the complexity of ecological interactions and evolutionary mechanisms.

INTRODUCTION

Since Lamarck's early ideas and Darwin's groundbreaking theory of natural selection, evolution has captivated biologists for over 200 years, sparking debates and ever-going research that continue to shape and evolve the field to this day.[1,2] An example of topics of intense study and widespread interest lies in evolutionary radiation, the rapid burst of diversification, which is a fundamental component of evolution and likely the source of the incredible biodiversity we see today.[3] These radiations can arise through both adaptive (ecological opportunity and natural selection) and non-adaptive processes (genetic drift and geographic isolation).[4–6] When adaptive processes prevail, adaptive radiation leads to the rapid evolution of new lifeforms adaptively exploiting various ecological niches. This diversification into novel ecological roles is triggered by ecological opportunities arising from the relaxation of biotic pressures (i.e., competition and predation), this release granting access to untapped resources.[7–11] Many examples of such adaptative radiations have been studied, including cichlids,[12–14] Darwin's finches,[15,16] Hawaiian honeycreepers,[17,18] and Anolis lizards[19]; however, there are very few examples from the marine realm.[20–23]

Researchers have long studied the causes and consequences of adaptive radiations to better understand the mechanisms governing species diversification.[6] Despite the significant and ongoing scientific interest in adaptive radiation as a fundamental source of biodiversity, many aspects of its drivers and dynamics

remain unexplored. While it is well established that individual speciation events can occur rapidly under certain conditions, we often struggle to explain the rapid speciation events that happen in quick succession within a single lineage.

Understanding evolutionary radiations is challenging because the original opportunities triggering these events are often poorly defined. Additionally, our ability to precisely characterize the ecological, morphological, and physiological differences among species produced by radiation is often limited, particularly for aquatic species living in environments where long-term studies are more difficult. Consequently, aside from iconic cases such as cichlids,[12–14] our comprehension of the processes and patterns of adaptive radiation remains relatively limited.

Anemonefishes (genus *Amphiprion*) are a group of 28 species within the Pomacentridae (damselfish) family.[24,25] They are particularly well suited to the study of adaptive radiation for two main reasons: (1) the size of the radiation is relatively limited, allowing us to grasp the main types of species produced during the radiation, and (2) the initial trigger leading to their diversification, the establishment of mutualistic symbiosis with giant sea anemone is known.[23]

Anemonefish diverged from their free-living ancestors approximately 25–30 million years ago.[23] They evolved this symbiosis at least three times independently with each of the three major host anemone clades (*Stichodactylina*, *Hetreactina*, and *Entacmea*).[26,27] However, their adaptive radiation only occurred around 13.2 million years ago,[23] which, interestingly, coincides with the diversification of most host anemone species within each clade in the past 13 million years. Until recently, it was believed that the fish and anemone did not co-evolve,[27] but these recent findings suggest a potential co-diversification that may have facilitated the adaptive radiation of anemonefish.[28]

Anemonefish non-randomly associate with ten species of giant sea anemones.[26,29] The host specificity of this interaction is highly variable. Some species are strict specialists that associate with only one host (e.g., *A. biaculeatus* and *A. frenatus*). By contrast, others are generalists living in up to all ten species of giant host sea anemones (e.g., *A. clarkii*).[30,31] Others, such as *A. ocellaris*, are intermediates, having two to three hosts. Because different anemone species have different environmental preferences (depth, substrate, and current regime), anemonefish also have various levels of habitat specialization.[32] Within natural anemonefish assemblages, host preferences allow the coexistence of multiple fish species in the same area.[33–35] Habitat differentiation is thus not only a driver of the diversification of anemonefish but also the main mechanism allowing the coexistence of multiple species. It has been proposed that following the acquisition of mutualism with sea anemones, anemonefish diversified into multiple ecological niches linked to host (i.e., host-specificity level) and environment (e.g., depth and substrate). According to this model, different anemonefish species developed convergent phenotypes correlated to their host-associated ecological niche.[23] Already in the early 1970s, it was suggested that anemonefish species could be classified into generalists or specialists given, of course, their number of hosts, but also the shape of their tail (emarginated vs. round), which relates to their swimming capacities (good swimmer or not), their body depth (deep-bodied vs. slender-bodied), and their dependence on the host for protection (low or high dependence).[36]

Swimming performance is crucial for the survival and fitness of aquatic animals, affecting dispersal, migration, habitat shifts, reproduction, and prey-predator interactions.[37–39] It is, therefore, of substantial ecological importance and is thought to undergo selection pressure that improves evolutionary fitness.[40–42] For anemonefish, transitioning to a symbiotic life with large benthic cnidarians likely required adaptations in body shape and swimming capabilities due to the reduced need for rapid swimming.[23,43] *Amphiprion* species that associate with many hosts or live in deeper environments tend to be bigger and are hypothesized to be better swimmers.[23] It was also hypothesized that three-banded anemonefish with indented dorsal fins are poorer swimmers than those with continuous dorsal fins.[44] However, to the best of our knowledge, none of the above-mentioned associations have ever been experimentally tested.

Here, we aim to empirically test for the existence of eco-morphotypes within anemonefish related to swimming capabilities and determine the main steps of their evolution. We focused on the swimming performances of six anemonefish species living in sympatry on Okinawa Island (Southern Japan), presenting various pigmentation patterns and levels of host specificity. Using a combination of field observations, swimming tunnel experiments, numerical simulations, and a series of morphological parameters, we indeed identified different eco-morphotypes based on their morphology, physiology, and ecology. Interestingly, these eco-morphotypes did not match the traditional view based on sea anemone host specificity. To generalize these observations, we collected a subset of our variables for eight additional species spread out in the anemonefish evolutionary tree. This allowed us to understand the evolutionary history of these eco-morphotypes and how different axes of diversification might have shaped the variety of anemonefish we observe today. Taken together, our analysis reveals an unsuspected fine-tuned diversification among anemonefish, providing an example of how natural selection precisely shapes biodiversity during these radiative bursts.

RESULTS

To better characterize the phenotypic differences existing between the various species of anemonefish, we performed a series of analyses exploring their dependence on their host (defined as the proportion of time they spend within their sea anemone) in natural conditions, their swimming abilities, and the cost associated with swimming, as well as their musculature. We performed this characterization on the six species from Okinawa (*Amphiprion clarkii*, *A. frenatus*, *A. ocellaris*, *A. perideraion*, *A. polymnus*, and *A. sandaracinos*), which present a variety of pigmentation patterns and host specificity levels (Figure S1) for which we can combine field and laboratory analysis. Then we generalize our observation by collecting morphological data in eight additional species, representative of the anemonefishes' diversity.

Anemonefishes have different levels of dependence on their host

To quantify the level of dependence of the six anemonefish species living in Okinawa, we performed *in situ* video recordings of five colonies of each species. Then, we assessed the time

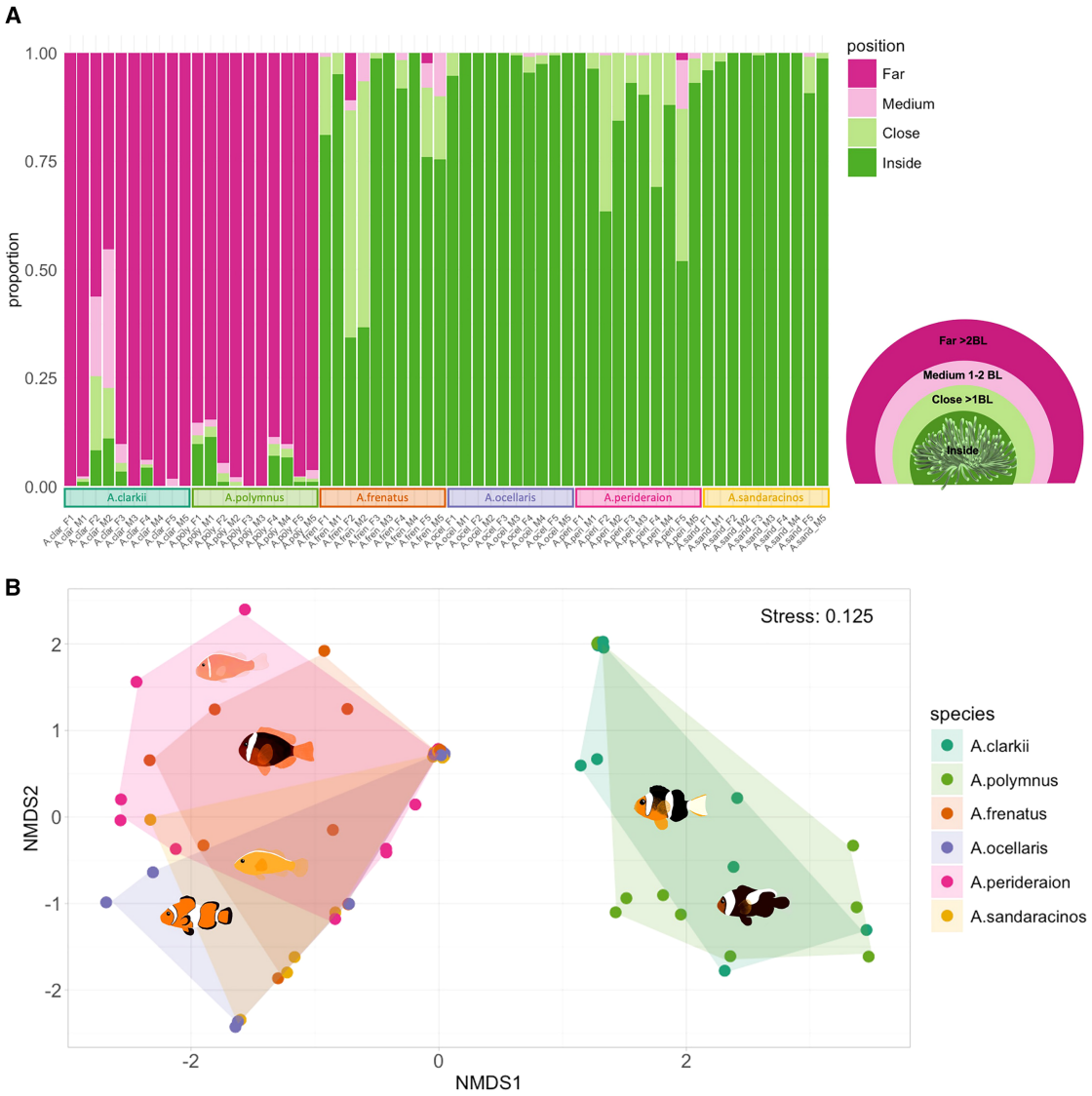

Figure 1. Anemonefish's dependence on their host is variable

(A) The stacked histogram represents host use (proportion of time spent in each area over a 10-min period) for each individual fish (averaged results by species are shown in Figure S2). The fish's position relative to its host was coded into four categories: inside the anemone or outside, with three levels: close, medium, and far. (B) nMDS on robust Aitchison distance matrix. The nMDS reflects how species differed in terms of habitat use. *A. clarkii* and *A. polymnus* individuals spent most of their time far from their anemone, while *A. ocellaris* and *A. sandaracinos* were almost always inside their host. *A. frenatus* and *A. perideraion* had slightly more variable behavior.

spent by the adult pair inside the host and at three different distances (close, medium, and far) from that host. The video recordings revealed differences in dependence among species (PERMANOVA $p < 0.0001$; Figure S2B) with consistent behavior among individuals (Figure 1A) and no difference between males and females within each species (Figures S2B and S2D).

We identified two main patterns of host use by the fishes. Two species (*A. clarkii* and *A. polymnus*) spent most of their time outside and relatively far from their host (respectively, 88.2% and 93.6% at more than two body lengths and only 2.8% and 3.8% inside the anemone). Some individuals would venture as far as not being visible in the camera field anymore. Conversely, the four other species would never or rarely venture outside of their host (80.3%, 98.6%, 82.9%, and 98.3% inside the anemone for *A. frenatus*, *A. ocellaris*, *A. perideraion*, and *A. sandaracinos*, respectively) (Figures 1A and S2). When visualizing similarities in host dependence (time spent in each distance category) between individuals using non-metric multidimensional scaling (nMDS), this distinction between "adventurer" and "homebody" is clearly visible along the first axis (Figure 1B). In the homebody group, further distinctions could be made between species always staying within their host (*A. ocellaris* and *A. sandaracinos*) and those with a slightly more variable behavior, sometimes venturing outside the anemone but within its close vicinity (*A. frenatus* and *A. perideraion*) (Figures 1A and S2). This trend is mainly reflected by the second

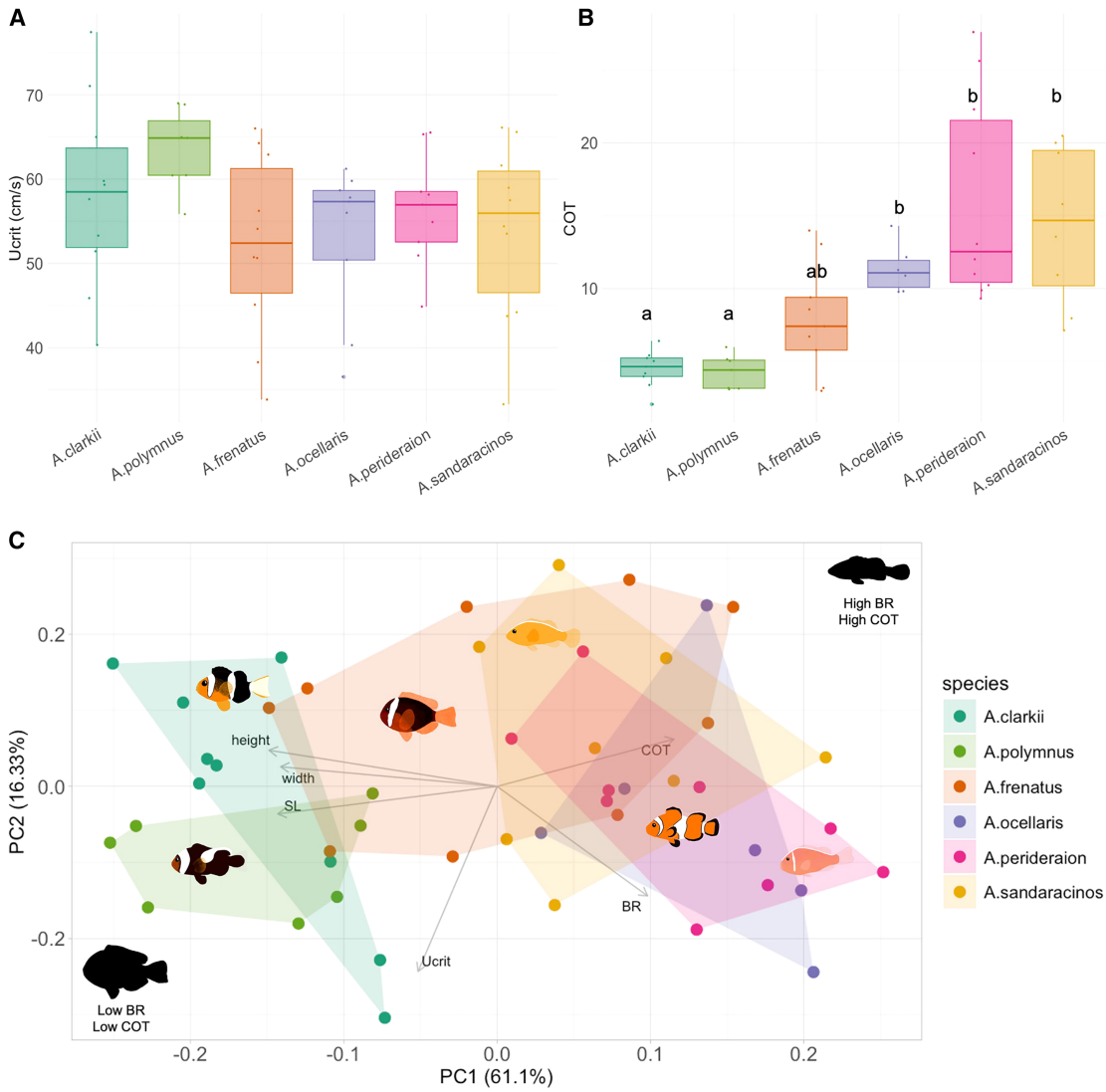

Figure 2. Anemonefish have similar swimming performances but different energy needs

The number of fish tested per species and variable can be found in Figure S3F.

(A) Boxplot of the critical swimming speed (U_{crit}) (in cm/s) showing the first and third quartiles (bottom and top of the box), median (middle horizontal bar), and minimal and maximal values (whiskers) for each species. Note that while differences are not significant, *A. clarkii* and *A. polymnus* seem to be able to achieve slightly higher speeds. Results for size-normalized speed (expressed in BL/s) are shown in Figure S3.

(B) Boxplot of the COT at U_{crit} (O_2 consumption per unit distance, dimensionless), notice the significant difference (species that are not sharing a letter differ significantly) between the lowest COT of *A. clarkii* and *A. polymnus* and the highest one of *A. sandaracinos*, *A. perideraion*, and *A. ocellaris*.

(C) PCA of U_{crit}, COT, and general morphological parameters of the fish (SL, standard length; height, widest dorsoventral axis; width, widest transverse axis; BR, body ratio height/SL). The first axis separates bigger species with low COT and BR on the left from smaller species with high COT and BR on the right. The second axis relates more to U_{crit}.

See also Table S1.

axis of the nMDS (Figure 1B). These differences in behavior did not seem to relate to either host specificity or pigmentation pattern. Indeed, *A. perideraion*, *A. ocellaris*, and *A. sandaracinos* cluster together while they have very different pigmentation patterns and various levels of host specificity. Similarly, *A. clarkii*, the most generalist species, showed a similar level of dependence to *A. polymnus*, a relatively specialist species (see Figure S1 for a detailed description of color pattern and host specificity).

Anemonefishes have different swimming capacities

We hypothesized that species with low host dependence would have better swimming capacities than those never venturing outside their host. To test this hypothesis, we conducted a critical swimming speed experiment associated with respirometry for the same six species. This allowed us to determine the critical speed (U_{crit}), a standard and ecologically relevant measure of swimming performance,[37,45] and estimate the standard metabolic rate (SMR, i.e., resting oxygen consumption), maximal

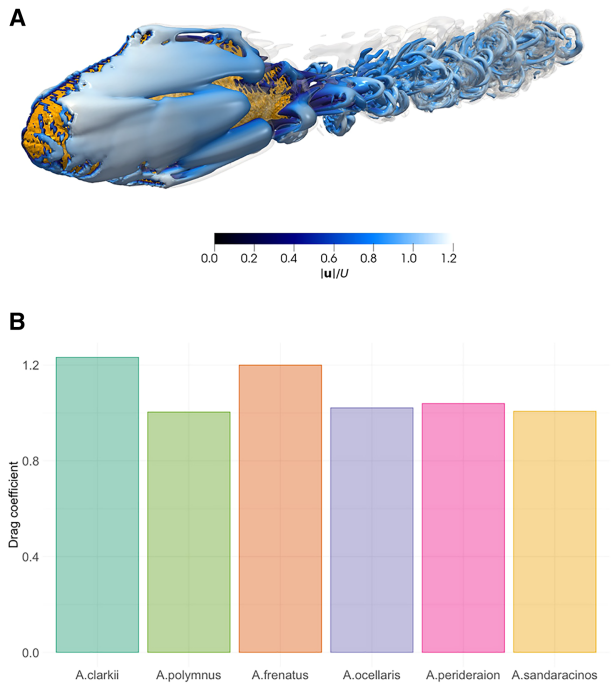

Figure 3. Anemonefish's drag coefficient is only slightly variable

(A) Example of the numerical simulation of the water flow over *A. ocellaris* at Reynolds number (Re) = 10^4, showing the instantaneous isosurfaces using the Q-criterion at two different levels: Q = 0.001 $(U/L)^2$ are in transparent gray, and Q = 5 $(U/L)^2$ are colored with the fluid velocity magnitude according to the colormap, i.e., from dark blue to white, and here, U is the free-stream velocity and L is the length/longitudinal extension of the fish.

(B) Drag coefficient at Re = 10^3. The histogram representation is for visual clarity and represents one value from the simulation for each species. Drag coefficient values are shown in Data S1.

metabolic rate (MMR, i.e., oxygen consumption during the maximum sustainable rate of exercise), aerobic scope (A.scope, i.e., the ability to increase oxygen uptake rate), and cost of transport (COT, i.e., the energetic cost of covering a unit distance) for each species.

The female anemonefish is usually bigger than the male.[46–48] As this sexual dimorphism was observed for all our experimental fish (Table S1) and could eventually affect speed and metabolism, we checked for differences between sexes for the various parameters. We found that despite a general trend for higher metabolism and relative speed (U_{crit} in $BL.s^{-1}$) in males, those differences were not significant. Thus, the following results consider both sexes together.

The experiments revealed a trend for higher U_{crit} (in $cm.s^{-1}$) in larger species, but surprisingly, no significant differences between species (Kruskal-Wallis chi-squared = 7.8305, df = 5, p = 0.1658; Figure 2A), which is probably due to high intraspecific variation. When standardized by length (expressed in $BL.s^{-1}$), smaller species tended to have higher U_{crit} but, again, with no significant difference (Figure S3). All speed values in cm/s and BL/s are reported in Figure S3F. On the other hand, metabolic parameters (SMR, MMR, A.scope, and COT) were significantly different among species. A general trend for a lower metabolism was observed in *A. clarkii* and *A. polymnus* when higher values were recorded in *A. perideraion*, *A. ocellaris*, and *A. sandaracinos* (Figures 2B and S3). Of particular interest are the differences in COT at U_{crit} (Kruskal-Wallis chi-squared = 32.3473, df = 5, p = 5.07e−6). Indeed, *A. clarkii* and *A. polymnus* needed significantly less energy to swim at their U_{crit} than *A. ocellaris*, *A. perideraion*, and *A. sandaracinos*. *A. frenatus* had an intermediate COT (Figure 2B). This trend was also observed when the COT was calculated for U_{crit} expressed in $BL.s^{-1}$ (Figure S3). This result indicates that even if able to swim at the same speed, achieving such a speed will cost much more energy to some species (*A. ocellaris*, *A. perideraion*, and *A. sandaracinos*) than to others (*A. clarkii* and *A. polymnus*).

Interestingly, a principal-component analysis (PCA) performed on these physiological and functional traits (Figure 2C) revealed a grouping similar to that previously observed for the host dependence shown in Figure 1B: *A. clarkii* and *A. polymnus* cluster together on the left side, while *A. ocellaris*, *A. peridarion*, and *A. sandarcinos* are on the right side of the physio-morphospace, and *A. frenatus* overlaps both groups (Figure 2C). The first axis explains 61.1% of the variation in the data. It separates mainly large individuals with low COT and body ratio (BR) from smaller ones with higher COT and BR, suggesting an effect of the fish morphology on the COT. The second axis, which accounts for 16.33% of the variation, seems to relate mainly to U_{crit}.

Combining U_{crit} with metabolic and morphological measurements, we could, therefore, identify two main groups in anemonefish swimming capacities. Bigger, deep-bodied species with lower swimming-related energy needs on one side and smaller, slender species with higher swimming-related energy needs on the other. Interestingly, this grouping is consistent with host dependence while having no apparent association with host specificity or pigmentation pattern.

Eco-morphotypes can be defined based on swimming capacities and morphology

It has been suggested that body shape is one of the main factors influencing swimming performance.[45,49,50] At first sight, anemonefish have quite different shapes, from damselfish-looking *A. clarkii* to elongated skunks (e.g., *A. sandaracinos*), and the above results suggest that those differences in shape could somehow relate to the COT and the general swimming behavior of anemonefishes (Figure 2C). As body shape influences the hydrodynamical constraints (e.g., drag) experienced by the fish, which in turn can influence its swimming performance and metabolism, we estimated the drag coefficient of the six same anemonefish species. For this, we scanned an individual of each of the six species by micro-computed tomography (μCT) to precisely reconstruct their surface. We used these images to input geometry and perform computational fluid dynamics simulations (STAR Methods). These simulations revealed an overall similar drag coefficient (around 1) among the different species (Figure 3), with, surprisingly, a slight deviation observed for *A. clarkii* and *A. frenatus*, having a larger drag coefficient (around 1.2). Given that the selected Reynolds number was the same for all species, such deviation could be ascribed to geometrical differences (e.g., lower BR).

The above result was quite unexpected since species with lower COT experienced a larger drag. Therefore, we looked at myology, which is well known to influence swimming

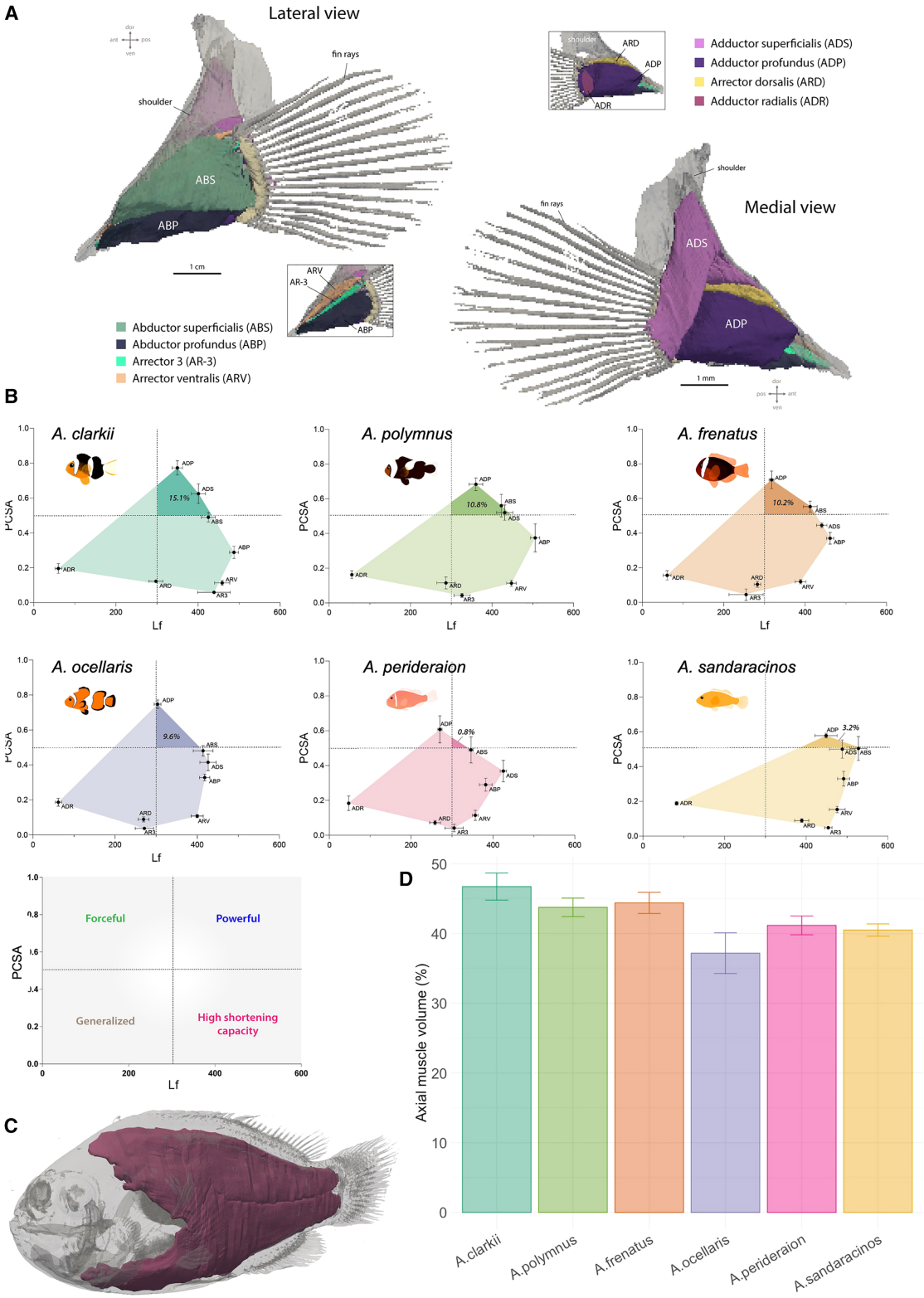

Figure 4. Anemonefishes have different muscle morphology

(A) 3D representation of the segmented pectoral fin muscles. Visualizations for each species are shown in Figure S4.

(B) Functional space plot of pectoral fin muscles (ABP, abductor profundus; ABS, abductor superficialis; ADP, adductor profundus; ADS, adductor superficialis; ADR, adductor radialis; ARD, arrector dorsalis; ARV, arrector ventralis; and AR-3, arrector 3) for the six studied anemonefish species. The fiber length (L_f, *x* axis,

(legend continued on next page)

performance.[38,51,52] From three μCT scans per species, axial and pectoral fin muscles were segmented and compared among species (Figures 4 and S4). Physiological cross-sectional area (PCSA, a proxy of the force-generating capacity of a muscle) for each pectoral fin muscle was plotted against fiber length (i.e., the muscle's working range). These muscle properties are especially important parameters of muscle architecture and serve as proxies to infer muscle function. The generated functional space plot can be used to compare muscle force production between species and to explore the trade-offs between potential force generation and working range capacities (i.e., relative muscle function; see STAR Methods and Ziadi-Künzli et al.[53] for more details) (Figure 4B).

The distribution of pectoral fin muscles among species consistently occupies three of the four quadrants in the functional space plot: "generalized" muscles (weak/slow), muscles with high "shortening capacities" (fast), and "powerful" muscles (strength and speed) (Figure 4B). The adductor profundus (ADP) has the highest PCSA, marking it as the most powerful muscle (Figures 4A and 4B). Its combined action with the deep and superficial adductor muscles (abductor profondus [ABP] and abductor superficialis [ABS]) facilitates fin extension during the propulsive phase. Fine-tuning of fin movement occurs through muscles with the longest fibers, like the deep and superficial abductors (ABP, ABS) (Figures 4A and 4B). The adductor radialis (ADR) is the weakest muscle, with low PCSA and short fibers (Figure 4B).

The main difference among species lies in the presence of powerful muscles (located in the upper right quadrant), which include the ADP for all species (but *A. perideraion*) and also the ABS and the adductor superficialis (ADS) for some species (Figure 4B). For example, *A. clarkii* exhibits these muscles in approximately 15% of the functional space plot area, whereas *A. polymnus*, *A. ocellaris*, and *A. frenatus* show a smaller proportion, around 10%, and *A. sandaracinos* even less, at 3.2%. *A. perideraion* stands out for lacking powerful fin muscles, registering at a mere 0.8% (Figure 4B).

Minor differences were also noted in axial muscle proportions, with percentages ranging from just over 37.2% in *A. ocellaris* to 46.7% in *A. clarkii* (Figure 4D). Muscle volumes and drag coefficients for each species are summarized in Data S1.

Those results confirm the grouping of *A. polymnus* and *A. clarkii* on one hand and *A. ocellaris*, *A. perideraion*, and *A. sandaracinos* on the other. The two groups are clearly visible in the first axis of the PCA (explaining 55.25% of variance), while *A. frenatus* has an intermediate position in the morphospace (Figure 5). This axis mainly relates to the COT, BR, and proportions of axial and powerful fin muscles. The second axis explains 24.96% of the variance and separates *A. polymnus*, *A. ocellaris*, and *A. sandaracinos* at the bottom from *A. clarkii*, *A. frenatus*, and *A. perideraion* at the top. This seems to relate mainly to the drag and the volume of the main pectoral fin muscles.

Together, our results suggest the existence of two main eco-morphotypes. On one side, fish with large muscles and a lower metabolism are equipped for swimming and venture outside their host anemone. On the other side, fish with smaller muscles and higher metabolisms rarely or never leave their host. An intermediate phenotype was observed for *A. frenatus*, which could represent a third eco-morphotype. In some regards, those eco-morphotypes partially match the hypothesized ones, as species with a deep body have better swimming capacities and lower host dependence than those with a slender body. However, we again could not identify any link between swimming capacities and either pigmentation pattern or host specificity.

The diversification of swimming-related morphological traits happened independently of host specificity

After revealing swimming eco-morphotypes in anemonefish from Okinawa Island, we aimed to explore the evolution of these morphologies across a larger phylogenetic sample of *Amphiprion* species. To do so, we collected a subset of the variables considered above (muscle volumes, drag coefficient, and BR; see Data S1 and Figure S5 for details) for eight additional species distributed over the anemonefish evolutionary tree and presenting a variety of pigmentation patterns and host specificity (Figure S1).

We first performed a PCA to reveal any structure in the morphospace and recovered a similar trend as with the six species from Okinawa, confirming the eco-morphotypes we previously defined. Species are distributed along PC1 (46.71%) according to the volume of their muscles, reflecting their swimming abilities and dependence on their host. From species expected to have poor swimming abilities and high dependence on their hosts (left side of the morphospace), such as *A. perideraion* and *A. biaculeatus*, to those expected to have better swimming performances and be less dependent on their host (right side of the morphospace), such as *A. ephippium* and *A. bicinctus*. Interestingly, several species (e.g., *A. chrysopterus* and *A. nigripes*) show an intermediate phenotype similar to that of *A. frenatus*, suggesting that phenotypic variation does not fall into two strictly discrete categories but rather forms a continuum. Of note is also the unusual case of *A. percula*, which strongly diverges from its sister species (*A. ocellaris*) despite the apparent similarity in body shape and ecology. PC2 (20.86%) separates species according to their drag coefficient and BR (Figure 6A).

We then qualitatively investigated the diversification of swimming eco-morphotypes by mapping the PC axes on the anemonefish phylogenetic tree.[54] Our ancestral state reconstruction, coupled with the mapping of traits, reveals the presence of convergence and divergence in aspects of swimming morphologies across the evolution of anemonefishes (Figure 6B). For example, the sister species *A. sandaracinos* and *A. perideraion* show similar trait values (PC1) to species belonging to the clade containing *A. biaculeatus* and *A. ocellaris*, while *A. percula* diverges from other species in its clade. Interestingly, the

mean ± SE) reflects a muscle's excursion or "working range." It is plotted against the PCSA (*y* axis, mean ± SE), which is directly proportional to the force-generating capacities of a given muscle. The graph at the bottom provides information on how to interpret this type of plot. The distribution of the muscles between species is similar, but notice the differences in the occupation of the top right corner (darker shade, corresponding to powerful muscles).
(C) 3D representation of the segmented axial muscles (myotomes).
(D) Histogram of the volume of axial muscles (mean ± SE).
See also Data S1.

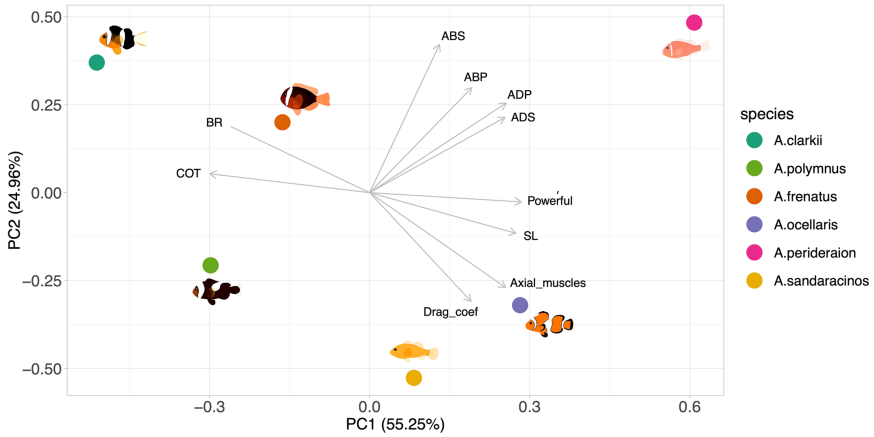

Figure 5. Eco-morphotype can be defined using morphological, physiological, and behavioral traits

Species are mainly divided into two groups (first axis): (1) bigger species with higher muscle volume and lower COT with negative values (note they are also those spending the most time outside their host) and (2) smaller, more elongated species with lower muscle volume and higher COT with positive values (note they are also those spending most of their time inside their host). The second axis seems to relate mainly to the drag coefficient. Details on drag coefficient and muscle volumes, together with functional space plots, for additional species are provided in Figure S5. BR, body ratio; SL, standard length; COT, cost of transport; powerful, surface of the top right quadrant of the functional space plot; ABS, volume of the abductor superficialis; ABP, volume of the abductor profondus; ADP, volume of adductor profondus; ADS, volume of the adductor superficialis.

distribution of traits across the phylogeny suggests that the majority of derived lineages (e.g., *A. polymnus*) evolved to different swimming eco-morphotypes than the most basal lineages (*A. biaculeatus* and *A. ocellaris*) (Figure 6B).

We then used phylogenetic generalized least squares (PGLSs) models to investigate if the evolution of swimming morphologies (using the same traits as for the PCA) and host specificity (i.e., the use of different sea anemones) were correlated. The best linear model, i.e., a PGLS analysis assuming an Ornstein-Uhlenbeck model (GIC_{OU} = 63.1 < GIC_{OLS} = 64.1 < GIC_{BM} = 66.5 < GIC_{EB} = 68.5), strongly supported an absence of evolutionary relationship between morphological traits associated with swimming and host specificity (Wilks' Lambda = 0.65, p = 0.63). Confirming our qualitative assessment, this last result highlights that anemonefish diversification occurred along several axes: host specificity and host dependence, the latter being tightly linked to swimming abilities.

DISCUSSION

By integrating different methods, we identified distinct eco-morphotypes in anemonefishes based on morphology, physiology, and ecology and showed that they emerged through convergence and evolved independently of host specificity, challenging the traditional generalist-specialist perspective. The combination of traits we quantified (host dependence, swimming speed, metabolism, drag coefficient, and muscle types and proportions) segregated species along a gradient, with, on one end, "poor swimmers" highly dependent on their host with low drag coefficient, low muscle proportion, and high COT and, on the other end, "good swimmers" venturing outside their host with high drag coefficient but high muscle proportion and low COT. These two categories have no direct relation to the number or species of host.

Even though we have not characterized all species from the clade, our sampling encompasses a broad range of morphological and ecological diversity found in *Amphiprion* and includes species distributed throughout the entire phylogenetic tree (Figure S1), providing a first functional characterization of different species of anemonefish.

An unsuspected diversity of swimming abilities

Anemonefish swimming performances have been hypothesized to vary according to habitat and host specificity, and members of the tribe are generally considered "bad swimmers," as it is assumed that the transition to symbiotic life caused the reduced necessity for rapid and sustained swimming, leading to adjustments in body shape and swimming capabilities.[23,43] Our study is actually the first to measure the swimming performances of multiple anemonefish species at the adult stage. Surprisingly, our results show performances comparable to that of other Pomacentridae and even similar to reef fish in general.[55] The swimming performances of anemonefish may thus not be as affected by symbiotic life as previously thought. Indeed, there are several pieces of evidence that some species can easily move several tens of meters.[56–59] Also, during their elaborate social life, anemonefish have numerous antagonistic interactions, chase each other, and even sometimes violently fight, which undoubtedly explains this need to maintain good swimming abilities. It will be useful to rigorously quantify interactions within a colony to better understand these needs.

Inter-individual variation in U_{crit} within species was high (up to 2.5-fold), which might explain the absence of significant differences among species. In fish, variations in swimming performance and metabolism are common between species but also at the population or even individual levels.[60,61] These variations can relate to morphological parameters, notably weight, length, and body and fin ratios,[60,61] as well as parameters such as genotype, developmental conditions, or even personality.[62] As anemonefish have a long life span,[63] age could also be another influencing factor, as it correlates to declining performances and physiological functions in humans.[64,65] Whatever the underlying mechanism linked to this variability, even if not statistically significant, the trends observed in this study are well-marked and might reflect relevant biological and ecological differences among species. Body shape and muscle ratio are usually positively correlated to U_{crit}, and slender fish with a high proportion of muscle can reach

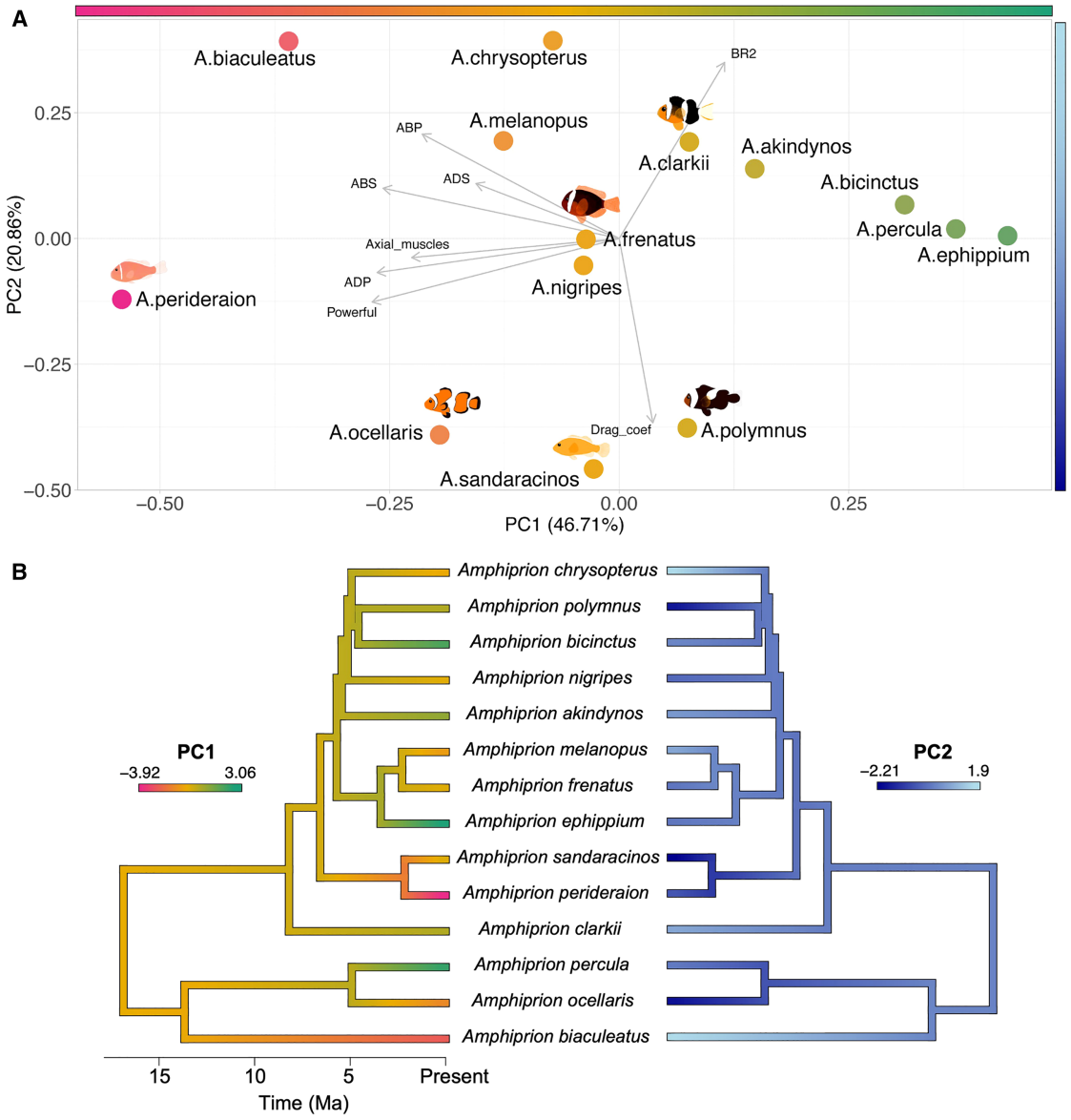

Figure 6. Evolutionary dynamics of swimming eco-morphotypes

(A) PCA of morphological traits and drag coefficient for the set of 14 species. Species segregate along the first axis, which mainly relates to muscle volume. It separates the different anemonefishes according to a gradient of species with low swimming performances on the left side to those with high swimming performances on the right side. BR, body ratio; SL, standard length; COT, cost of transport; powerful, surface of the top right quadrant of the functional space plot; ABS, volume of the abductor superficialis; ABP, volume of the abductor profondus; ADP, volume of adductor profondus; ADS, volume of the adductor superficialis.

(B) Mapping of PC1 and PC2 on the anemonefish phylogenetic tree.

higher speeds as they can generate more thrust.[49,66] We found partly conflicting results, as the species with the lower BR and the higher drag (such as *A. clarkii* and *A. frenatus*) performed as well or even better than slender species (for example, *A. perideraion* and *A. sandaracinos*). They, however, have a higher axial muscle proportion and more powerful pectoral fin muscles, which might provide some compensation for their high drag. The hydrodynamic disadvantage experienced by deep-bodied species might also be compensated for with a lower metabolism (SMR and MMR), thus reducing their COT (as observed in *A. clarkii*, *A. polymnus*, and *A. frenatus*).[67] Finally, differences in swimming efficiency could also be influenced by swimming mode. Indeed, during the experiment, the fish used a combination of median-paired fin and body-caudal fin swimming at lower speeds and then transitioned to exclusive body-caudal fin swimming as the speed increased (personal observations). As undulatory swimming is more costly than median-paired fin swimming, the timing of this transition and the amplitude of the undulatory motion during body-caudal fin swimming could also influence energetic cost and swimming performance.[55,68]

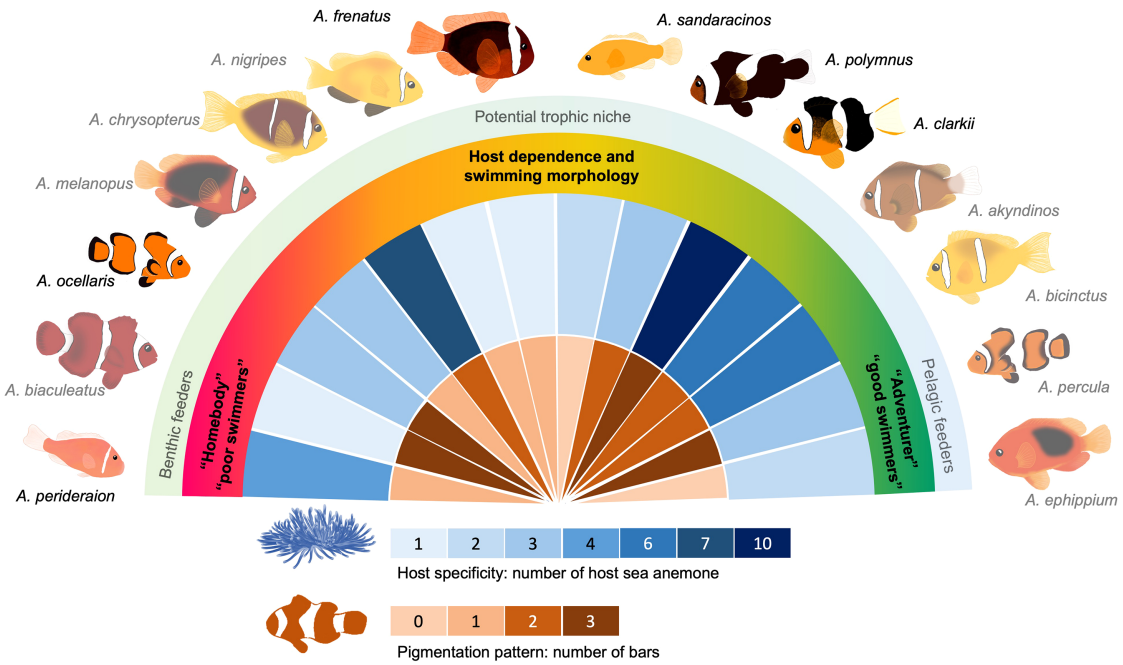

Figure 7. Model of the diversification of anemonefishes along multiple axes

General model of the radiation of anemonefishes along multiple axes: pigmentation pattern (signaling), host specificity (macro-habitat use), and swimming capacities (micro-habitat use and potentially trophic niche). Note how each species presents a different combination of each of those axes. The model is presented for the studied species. Species that are fully opaque are those for which morphological, ecological, and physiological data were collected, and species in transparency are those for which only morphological data were collected. Number of host anemones, according to Fautin and Allen,[31] and pigmentation pattern, according to Salis et al.[44]

Swimming abilities can be measured in many ways, and measurements of U_{crit} and metabolic parameters in a swimming tunnel only give us a general overview. Indeed, such an artificial framework leaves aside certain aspects that are undoubtedly very important for these fish, like maneuverability or motivation. It will be necessary to develop more sensitive tests closely tied to the symbiotic life in colonies to achieve more accurate measurements. Nevertheless, these initial analyses already highlight a diversity of swimming abilities that had largely been underestimated until now. In the future, it will also be important to better understand the relationship between muscle anatomy, metabolism, and swimming capabilities—an objective that is undoubtedly achievable with these species, which are emerging as valuable models for Eco-Evo-Devo studies.[69,70]

Integrated eco-morphotypes and ecological implications

Our results suggest a link between anemonefish's phenotype (morphological and physiological traits) and their lifestyle in the reef. Indeed, species with a higher proportion of muscle and better swimming capacities are also less dependent on their host anemone. These differences in host dependence could result from various factors and influence ecological interactions at different levels. For example, variations in host dependence could reflect differences in trophic niches, and adventurer species could be more planktivorous (e.g., *A. clarkii*), while the homebody could be more benthic feeders (e.g., *A. akallopisos*[71]). Similarly, Litsios et al. hypothesized that generalist anemonefish species, having more gill rakers, would rely more on planktonic prey than specialist ones.[23] However, a previous study found that out of eight *Amphiprion* species, seven were pelagic feeders.[72] These seven species include *A. clarkii*, *A. frenatus*, *A. perideraion*, and *A. sandaracinos*, which showed different host dependence levels and have different host specificity. It must be stressed that anemonefish's diet remains surprisingly understudied, and further investigation of their trophic ecology would help to understand their diversification and the functional role they play in the reef community.

The metabolic status of the fish can also influence fish behavior at the individual level[73,74]; thus, it is possible that the same phenomenon also happens at the interspecific level, driving behavioral differences (e.g., boldness/shyness) between species with different metabolism and swimming abilities. In turn, the fish's behavior can influence the strength of the mutualistic interaction with the host anemone (i.e., how beneficial it is for the anemone in terms of growth). Indeed, a study on *A. percula* showed that anemone's growth was positively correlated to fish shyness (measured as the time spent within one body length of the anemone).[75] Again, this effect results from inter-individual variation within the same species. Given the amplitude of the variations in time spent within the anemone between species observed in this study, it is reasonable to think that fish species with different behaviors might have a different influence on their host.[76] Performing more detailed studies of time allocation (e.g., feeding, reproduction, tending to the host, etc.) for different fish species would help us understand how the fish behavior influences the anemone's fitness.

Differences in host dependence between anemonefish species might also play a key role in other interspecific interactions,

notably cohabitation between anemonefish species. Cohabitating anemonefish (two different species living in the same host forming an interspecific group) have different pigmentation patterns (number of bars), which is assumed to help species recognition and avoid competition.[35,44,77] Combinations of species are, however, independent of body size, phylogenetic relatedness, and host specificity level.[78] Cohabitation is instead facilitated by lower aggressiveness and different spatial use of the host by cohabitating species.[78] Interestingly, reported pairs of cohabitating species always include species occupying two very different positions on the low-to-high swimming performance gradient detected in this study (e.g., *A. clarkii*/*A. perideraion*, *A. clarkii*/*A. sandaracinos*, and *A. melanopus*/*A. biaculeatus*), suggesting the importance of the studied behavioral, morphological, and physiological traits in sustaining cohabitation, as already mentioned in a previous study.[79]

Within natural anemonefish assemblages, niche differentiation (i.e., host preference and different habitats) is the main mechanism through which multiple fish species coexist in the same area.[33–35] Furthermore, in some cases (mainly in highly diverse systems), cohabitation seems to be an important process in maintaining anemonefish diversity. Understanding how multiple species coexist is a key focus in ecology. Yet despite extensive research in phenotypic trait variation between coexisting species, determining the relative importance of each niche component (e.g., resource partitioning, behavioral specialization, etc.) remains challenging.[80–82] On the other hand, cohabitation may also reduce anemonefish diversity by increasing the probability of hybridization, which can lead to genetic homogenization. Thus, the net effect of cohabitation on species diversity likely depends on the balance between these opposing processes.[83–85] Mutualist guilds are great model systems to investigate the mechanisms underlying species coexistence.[82] Anemonefish communities represent a perfect case study in the marine realm for which our study stresses the importance of considering multiple functional traits to grasp the complexity of mechanisms underlying the emergence and maintenance of diversity. Indeed, the phenotype of an organism is a complex whole, and we must be cautious not to overemphasize certain traits simply because they are more familiar to us. As our study highlights, particularly in marine organisms, it is challenging to quantitatively assess the phenotype and highlight the adaptive value of each trait. Often, we overlook critical aspects by focusing only on the obvious. A particularly striking example in our study is *A. percula*. It morphologically looks very similar to its sister species, *A. ocellaris*, and establishes symbiosis with the same species of host anemones, but our results show very different muscle volume. We also have growing evidence that the two species might have different developmental trajectories (authors' personal observation), suggesting they could be much more different than previously thought and stressing the need for further investigation. Our findings emphasize that while the number and quality of anemonefish hosts are important, other factors—such as swimming abilities, metabolic costs, and likely many others yet to be discovered—must also be considered.

A tentative model for the adaptive radiation of anemonefish

To date, most studies devoted to the diversification of anemonefishes focused on host specificity,[23,86] overlooking other potential axes of diversification. Yet ecological diversification is not always obvious, and diversification can happen along several axes. In adaptive radiation, diversification typically happens in stages: first in macro-habitat use, then in trophic niches, and finally, in signaling.[11,12,87,88] This pattern is seen in anemonefishes, with diversification happening according to host specificity (i.e., macro-habitat),[23] pigmentation pattern (i.e., signaling),[44] and as this study shows, host dependence and swimming performances. The lack of correlation between the studied morphological traits and host specificity builds up our understanding of anemonefish evolution by revealing a new axis of diversification that could relate to trophic niches and/or micro-habitat use. Our results reveal the diversification of swimming-related traits in anemonefish, producing convergent swimming eco-morphotypes over evolutionary time. However, the convergence observed may be only partial. The continuum of phenotypes we report suggests that gradual evolution along certain functional axes, combined with partial convergence of specific traits, could have filled the morphospace without clear discrete peaks.[89–91] This pattern may reflect the modular nature of trait evolution, with different traits diverging or converging at different times. The evolutionary history of anemonefish also includes multiple hybridization events[84] that might have contributed to their adaptive radiation. Also, gene flow and introgression could have played a role in shaping similar phenotypes. The resulting patterns from such processes could resemble that of convergence. We therefore ask for future studies with larger taxon sampling to explicitly test the convergent hypothesis.[92] Theories suggest that eco-morphological diversification happens quickly in the early stages of adaptive radiation and slows down as available niches become occupied.[11,93] Different traits can diversify at varying rates and times throughout the evolutionary history of a radiation, sometimes following the stepwise process mentioned earlier[12] or sometimes occurring in an iterative way.[94] In any case, the diversification of traits related to swimming abilities may have contributed to finer-scale habitat partitioning after other niches were already filled. Following the initial key physiological adaptation allowing the mutualistic symbiosis with giant sea anemones, we observed the small clade of anemonefish radiated along multiple axes, including host specificity, swimming capabilities, signaling, and probably diet adaptation. This evolutionary scenario follows the classic view of an adaptive radiation, making anemonefishes a new textbook example (Figure 7).

Adaptive radiation is an extensively studied phenomenon, but its drivers and dynamics remain untested in most cases. For example, the genetic basis of anemonefishes' radiation is well studied,[23,84,86,95] but trait utility has so far never been tested. Our study provides the first functional characterization of a wide diversity of anemonefish. Using an integrative approach, we revealed different ecological strategies independent of host specificity, translating into morphological and physiological differences, certainly understudied axes of diversification. Our results challenge the traditional specialist vs. generalist dichotomy, highlighting the complex nature of ecological interactions and evolutive mechanisms and the need for more functional and empirical studies for their better understanding.

A terminological conclusion

Lastly, it is interesting to note that species of the genus *Amphiprion* have two common English names: "anemonefish"

and "clownfish." Each name emphasizes different but complementary characteristics of these fish, highlighting a duality in their analysis. As anemonefish, they exhibit a remarkable ability to live in symbiosis with giant sea anemones. As clownfish, they display vibrant colors and a distinctive, seemingly joyful but actually grumpy and fidgety swimming style. Until now, studies on the evolutionary radiation of these fish have focused primarily on their characteristics as anemonefish. However, our study suggests that these fish are indeed "clowns" in a biological sense—a complex and finely integrated set of "Panglossian" phenotypic traits (perceived as optimal) likely facilitated their diversification.

RESOURCE AVAILABILITY

Lead contact

Requests for further information and resources should be directed to and will be fulfilled by the lead contact, Manon Mercader (manon.mercader@oist.jp).

Materials availability

μCT scans generated in this study are available at https://doi.org/10.5061/dryad.70rxwdc73 (6 Okinawan species, others will be provied on demand).

Data and code availability

- Data from the respirometry experiment are available in Table S1.
- Any other data reported in this paper will be shared by the lead contact upon request.
- Codes for computational simulation of water flow are available at https://www.oist.jp/research/research-units/cffu/fujin.
- Any additional information required to reanalyze the data reported in this paper is available from the lead contact upon request.

ACKNOWLEDGMENTS

The authors would like to thank Hiroki Takamiyagi, Keishu Asada, and Jeffrey Jolly for their help in the field; Tim Ravasi for providing the swimming tunnel; Billy Moore for his help with the respirometry experiment; Lilian Carlu for his great work maintaining the fish; and Nobuo Ueda (OIST Marine Sciences Station) for his help setting up equipment. They are also very grateful to the following for providing fish specimens: Shu-Hua Lee, Manuel Aranda and Holger Anlauf, Fabio Cortesi and Abigail Shaughnessy, David Lecchini and Frédéric Bertucci, Hui-Min Chung and Cooper Catalini, Richard Crowe, and Kei Miyamoto. They would like to warmly thank Ken Maeda for his advice on fish fixation and his help with museum specimens and Laurie Mitchell for his comments on the manuscript. Finally, they thank the Okinawa Institute of Science and Technology for funding.

AUTHOR CONTRIBUTIONS

Conceptualization, M.M., V.L., B.F., and F.Z.-K.; data curation, M.M., F.Z.-K., and S.O.; formal analysis, M.M., F.Z.-K., S.O., M.E.R., and B.F.; funding acquisition, V.L.; investigation, M.M., F.Z.-K., S.O., B.F., and S.K.; methodology, M.M., F.Z.-K., S.O., and B.F.; project administration, M.M. and V.L.; resources, V.L., M.E.R., F.Z.-K., and S.K.; supervision, V.L. and M.E.R.; visualization, M.M., S.O., F.Z.-K., and B.F.; writing – original draft, M.M., V.L., F.Z.-K., S.O., and B.F.; writing – review and editing, M.M., V.L., F.Z.-K., S.O., B.F., M.E.R., and S.K.

DECLARATION OF INTERESTS

The authors declare no competing interests.

STAR★METHODS

Detailed methods are provided in the online version of this paper and include the following:

SUPPLEMENTAL INFORMATION

Supplemental information can be found online at https://doi.org/10.1016/j.cub.2025.06.041.

Received: November 29, 2024
Revised: May 8, 2025
Accepted: June 18, 2025
Published: July 10, 2025

REFERENCES

1. Koonin, E.V., and Wolf, Y.I. (2009). Is evolution Darwinian or/and Lamarckian? Biol. Direct *4*, 42. https://doi.org/10.1186/1745-6150-4-42.
2. Laland, K., Uller, T., Feldman, M., Sterelny, K., Müller, G.B., Moczek, A., Jablonka, E., Odling-Smee, J., Wray, G.A., Hoekstra, H.E., et al. (2014). Does evolutionary theory need a rethink? Nature *514*, 161–164. https://doi.org/10.1038/514161a.
3. Simões, M., Breitkreuz, L., Alvarado, M., Baca, S., Cooper, J.C., Heins, L., Herzog, K., and Lieberman, B.S. (2016). The evolving theory of evolutionary radiations. Trends Ecol. Evol. *31*, 27–34. https://doi.org/10.1016/j.tree.2015.10.007.
4. Rundell, R.J., and Price, T.D. (2009). Adaptive radiation, nonadaptive radiation, ecological speciation and nonecological speciation. Trends Ecol. Evol. *24*, 394–399. https://doi.org/10.1016/j.tree.2009.02.007.
5. Matsubayashi, K.W., and Yamaguchi, R. (2022). The speciation view: Disentangling multiple causes of adaptive and non-adaptive radiation in terms of speciation. Popul. Ecol. *64*, 95–107. https://doi.org/10.1002/1438-390X.12103.
6. Losos, J.B. (2010). Adaptive radiation, ecological opportunity, and evolutionary determinism. Am. Nat. *175*, 623–639. https://doi.org/10.1086/652433.
7. Glor, R.E. (2010). Phylogenetic insights on adaptive radiation. Annu. Rev. Ecol. Evol. Syst. *41*, 251–270. https://doi.org/10.1146/annurev.ecolsys.39.110707.173447.
8. Simpson, G.G. (1953). The Major Features of Evolution (Columbia University Press). https://doi.org/10.7312/simp93764.
9. Givnish, T.J. (2015). Adaptive radiation versus 'radiation' and 'explosive diversification': why conceptual distinctions are fundamental to understanding evolution. New Phytol. *207*, 297–303. https://doi.org/10.1111/nph.13482.
10. Schluter, D. (2000). The Ecology of Adaptive Radiation (Oxford University Press). https://doi.org/10.1093/oso/9780198505235.001.0001.
11. Gavrilets, S., and Losos, J.B. (2009). Adaptive radiation: contrasting theory with data. Science *323*, 732–737. https://doi.org/10.1126/science.1157966.

12. Ronco, F., Matschiner, M., Böhne, A., Boila, A., Büscher, H.H., El Taher, A., Indermaur, A., Malinsky, M., Ricci, V., Kahmen, A., et al. (2021). Drivers and dynamics of a massive adaptive radiation in cichlid fishes. Nature *589*, 76–81. https://doi.org/10.1038/s41586-020-2930-4.

13. Seehausen, O. (2006). African cichlid fish: a model system in adaptive radiation research. Proc. Biol. Sci. *273*, 1987–1998. https://doi.org/10.1098/rspb.2006.3539.

14. Seehausen, O. (2015). Process and pattern in cichlid radiations – inferences for understanding unusually high rates of evolutionary diversification. New Phytol. *207*, 304–312. https://doi.org/10.1111/nph.13450.

15. Almén, M.S., Lamichhaney, S., Berglund, J., Grant, B.R., Grant, P.R., Webster, M.T., and Andersson, L. (2016). Adaptive radiation of Darwin's finches revisited using whole genome sequencing. BioEssays *38*, 14–20. https://doi.org/10.1002/bies.201500079.

16. Grant, P.R. (1981). Speciation and the adaptive radiation of Darwin's finches: The complex diversity of Darwin's finches may provide a key to the mystery of how intraspecific variation is transformed into interspecific variation. Am. Sci. *69*, 653–663.

17. Lerner, H.R.L., Meyer, M., James, H.F., Hofreiter, M., and Fleischer, R.C. (2011). Multilocus resolution of phylogeny and timescale in the extant adaptive radiation of Hawaiian honeycreepers. Curr. Biol. *21*, 1838–1844. https://doi.org/10.1016/j.cub.2011.09.039.

18. Navalón, G., Marugán-Lobón, J., Bright, J.A., Cooney, C.R., and Rayfield, E.J. (2020). The consequences of craniofacial integration for the adaptive radiations of Darwin's finches and Hawaiian honeycreepers. Nat. Ecol. Evol. *4*, 270–278. https://doi.org/10.1038/s41559-019-1092-y.

19. Butler, M.A., Sawyer, S.A., and Losos, J.B. (2007). Sexual dimorphism and adaptive radiation in Anolis lizards. Nature *447*, 202–205. https://doi.org/10.1038/nature05774.

20. Puebla, O. (2009). Ecological speciation in marine *v.* freshwater fishes. J. Fish Biol. *75*, 960–996. https://doi.org/10.1111/j.1095-8649.2009.02358.x.

21. Ingram, T. (2011). Speciation along a depth gradient in a marine adaptive radiation. Proc. Biol. Sci. *278*, 613–618. https://doi.org/10.1098/rspb.2010.1127.

22. Momigliano, P., Jokinen, H., Fraimout, A., Florin, A.-B., Norkko, A., and Merilä, J. (2017). Extraordinarily rapid speciation in a marine fish. Proc. Natl. Acad. Sci. USA *114*, 6074–6079. https://doi.org/10.1073/pnas.1615109114.

23. Litsios, G., Sims, C.A., Wüest, R.O., Pearman, P.B., Zimmermann, N.E., and Salamin, N. (2012). Mutualism with sea anemones triggered the adaptive radiation of clownfishes. BMC Evol. Biol. *12*, 212. https://doi.org/10.1186/1471-2148-12-212.

24. Quenouille, B., Bermingham, E., and Planes, S. (2004). Molecular systematics of the damselfishes (Teleostei: Pomacentridae): Bayesian phylogenetic analyses of mitochondrial and nuclear DNA sequences. Mol. Phylogenet. Evol. *31*, 66–88. https://doi.org/10.1016/S1055-7903(03)00278-1.

25. Tang, K.L., Stiassny, M.L.J., Mayden, R.L., and DeSalle, R. (2021). Systematics of Damselfishes. Ichthyol. Herpetol. *109*, 258–318. https://doi.org/10.1643/i2020105.

26. Titus, B.M., Benedict, C., Laroche, R., Gusmão, L.C., Van Deusen, V., Chiodo, T., Meyer, C.P., Berumen, M.L., Bartholomew, A., Yanagi, K., et al. (2019). Phylogenetic relationships among the clownfish-hosting sea anemones. Mol. Phylogenet. Evol. *139*, 106526. https://doi.org/10.1016/j.ympev.2019.106526.

27. Nguyen, H.-T.T., Dang, B.T., Glenner, H., and Geffen, A.J. (2020). Cophylogenetic analysis of the relationship between anemonefish *Amphiprion* (Perciformes: Pomacentridae) and their symbiotic host anemones (Anthozoa: Actiniaria). Mar. Biol. Res. *16*, 117–133. https://doi.org/10.1080/17451000.2020.1711952.

28. De Jode, A., Quattrini, A.M., Chiodo, T., Daly, M., McFadden, C.S., Berumen, M.L., Meyer, C.P., Mills, S., Beldade, R., Bartholomew, A., et al. (2024). Phylogenomics reveals coincident divergence between giant host sea anemones and the clownfish adaptive radiation. Preprint at bioRxiv. https://doi.org/10.1101/2024.01.24.576469.

29. Kashimoto, R., Rickards, E., Khalturin, K., and Laudet, V. (2024). Giant sea anemones. Curr. Biol. *34*, R481–R483. https://doi.org/10.1016/j.cub.2024.03.060.

30. Fautin, D.G. (1992). Anemonefish recruitment: the role of orders and chances. Symbiosis, 143–160.

31. Fautin, D.G., and Allen, G.R. (1997). Anemone Fishes and Their Host Sea Anemones: A Guide for Aquarists and Divers (Western Australian Museum).

32. Litsios, G., Kostikova, A., and Salamin, N. (2014). Host specialist clownfishes are environmental niche generalists. Proc. Biol. Sci. *281*, 20133220. https://doi.org/10.1098/rspb.2013.3220.

33. Elliott, J.K., Elliott, J.M., and Mariscal, R.N. (1995). Host selection, location, and association behaviors of anemonefishes in field settlement experiments. Mar. Biol. *122*, 377–389. https://doi.org/10.1007/BF00350870.

34. Elliott, J.K., and Mariscal, R.N. (2001). Coexistence of nine anemonefish species: differential host and habitat utilization, size and recruitment. Mar. Biol. *138*, 23–36. https://doi.org/10.1007/s002270000441.

35. Hayashi, K., Tachihara, K., and Reimer, J.D. (2018). Patterns of coexistence of six anemonefish species around subtropical Okinawa-jima Island, Japan. Coral Reefs *37*, 1027–1038. https://doi.org/10.1007/s00338-018-01740-1.

36. Allen, G.R. (1974). The Anemonefish: Their Classification and Biology, Second Edition (T.F.H. Publications Inc.).

37. Plaut, I. (2001). Critical swimming speed: its ecological relevance. Comp. Biochem. Physiol. A Mol. Integr. Physiol. *131*, 41–50. https://doi.org/10.1016/s1095-6433(01)00462-7.

38. Webb, P.W. (1975). Hydrodynamics and energetics of fish propulsion. Bull. Fish. Res. Board Can. *190*, 1–159.

39. Kapoor, B.G., and Domenici, P. (2010). Fish Locomotion: An Eco-ethological Perspective (CRC Press).

40. Reidy, S.P., Kerr, S.R., and Nelson, J.A. (2000). Aerobic and anaerobic swimming performance of individual atlantic cod. J. Exp. Biol. *203*, 347–357. https://doi.org/10.1242/jeb.203.2.347.

41. Wolter, C., and Arlinghaus, R. (2003). Navigation impacts on freshwater fish assemblages: the ecological relevance of swimming performance. Rev. Fish Biol. Fish. *13*, 63–89. https://doi.org/10.1023/A:1026350223459.

42. Priede, I.G. (1985). Metabolic scope in fishes. In Fish Energetics, P. Tytler, and P. Calow, eds. (Springer Netherlands), pp. 33–64. https://doi.org/10.1007/978-94-011-7918-8_2.

43. Elliott, J.K., Lougheed, S.C., Bateman, B., McPhee, L.K., and Boag, P.T. (1999). Molecular phylogenetic evidence for the evolution of specialization in anemonefishes. Proc. Biol. Sci. *266*, 677–685. https://doi.org/10.1098/rspb.1999.0689.

44. Salis, P., Roux, N., Soulat, O., Lecchini, D., Laudet, V., and Frédérich, B. (2018). Ontogenetic and phylogenetic simplification during white stripe evolution in clownfishes. BMC Biol. *16*, 90. https://doi.org/10.1186/s12915-018-0559-7.

45. Hammer, C. (1995). Fatigue and exercise tests with fish. Comp. Biochem. Physiol. A *112*, 1–20. https://doi.org/10.1016/0300-9629(95)00060-K.

46. Buston, P. (2003). Size and growth modification in clownfish. Nature *424*, 145–146. https://doi.org/10.1038/424145a.

47. Moyer, J.T., and Nakazono, A. (1978). Protandrous hermaphroditism in six species of the anemonefis genus Amphiprion in Japan. Japane J. Ichthyol. *25*, 101–106.

48. Fricke, H., and Fricke, S. (1977). Monogamy and sex change by aggressive dominance in coral reef fish. Nature *266*, 830–832. https://doi.org/10.1038/266830a0.

49. Ohlberger, J., Staaks, G., and Hölker, F. (2006). Swimming efficiency and the influence of morphology on swimming costs in fishes. J. Comp. Physiol. B *176*, 17–25. https://doi.org/10.1007/s00360-005-0024-0.

50. Lighthill, M.J. (1969). Hydromechanics of aquatic animal propulsion. Annu. Rev. Fluid Mech. *1*, 413–446. https://doi.org/10.1146/annurev.fl.01.010169.002213.

51. Videler, J.J. (1993). Fish Swimming (Springer Science & Business Media). https://doi.org/10.1007/978-94-011-1580-3.

52. Wardle, C.S., Videler, J.J., and Altringham, J.D. (1995). Tuning in to fish swimming waves: body form, swimming mode and muscle function. J. Exp. Biol. *198*, 1629–1636. https://doi.org/10.1242/jeb.198.8.1629.

53. Ziadi-Künzli, F., Maeda, K., Puchenkov, P., and Bandi, M.M. (2024). Anatomical insights into fish terrestrial locomotion: A study of barred mudskipper (*Periophthalmus argentilineatus*) fins based on μCT 3D reconstructions. J. Anat. *245*, 593–624. https://doi.org/10.1111/joa.14071.

54. McCord, C.L., Nash, C.M., Cooper, W.J., and Westneat, M.W. (2021). Phylogeny of the damselfishes (Pomacentridae) and patterns of asymmetrical diversification in body size and feeding ecology. PLoS One *16*, e0258889. https://doi.org/10.1371/journal.pone.0258889.

55. Fulton, C.J. (2007). Swimming speed performance in coral reef fishes: field validations reveal distinct functional groups. Coral Reefs *26*, 217–228. https://doi.org/10.1007/s00338-007-0195-0.

56. Hattori, A. (2005). High mobility of the protandrous anemonefish Amphiprion frenatus: nonrandom pair formation in limited shelter space. Ichthyol. Res. *52*, 57–63. https://doi.org/10.1007/s10228-004-0253-3.

57. Moyer, J.T. (1980). Influence of temperate waters on the behavior of the tropical anemonefish Amphiprion clarkii at Miyake-jima, Japan. Bull. Mar. Sci. 261–272.

58. Zwahlen, J., Mercader, M., and Laudet, V. (2024). Homing anemonefish: Amphiprion clarkii swim back to their original host after relocations. Mar. Biodivers. *54*, 80. https://doi.org/10.1007/s12526-024-01472-2.

59. Hattori, A. (1994). Inter-group movement and mate acquisition tactics of the protandrous anemonefish, Amphiprion clarkii, on a coral reef, Okinawa. Japane J. Ichthyol. *41*, 159–165. https://doi.org/10.11369/jji1950.41.159.

60. Rubio-Gracia, F., García-Berthou, E., Guasch, H., Zamora, L., and Vila-Gispert, A. (2020). Size-related effects and the influence of metabolic traits and morphology on swimming performance in fish. Curr. Zool. *66*, 493–503. https://doi.org/10.1093/cz/zoaa013.

61. Svozil, D.P., Baumgartner, L.J., Fulton, C.J., Kopf, R.K., and Watts, R.J. (2020). Morphological predictors of swimming speed performance in river and reservoir populations of Australian smelt *Retropinna* semoni. J. Fish Biol. *97*, 1632–1643. https://doi.org/10.1111/jfb.14494.

62. Burton, T., Killen, S.S., Armstrong, J.D., and Metcalfe, N.B. (2011). What causes intraspecific variation in resting metabolic rate and what are its ecological consequences? Proc. Biol. Sci. *278*, 3465–3473. https://doi.org/10.1098/rspb.2011.1778.

63. Buston, P.M., and García, M.B. (2007). An extraordinary life span estimate for the clown anemonefish Amphiprion percula. J. Fish Biol. *70*, 1710–1719. https://doi.org/10.1111/j.1095-8649.2007.01445.x.

64. Lazarus, N.R., Lord, J.M., and Harridge, S.D.R. (2019). The relationships and interactions between age, exercise and physiological function. J. Physiol. *597*, 1299–1309. https://doi.org/10.1113/JP277071.

65. Tanaka, H., and Seals, D.R. (2008). Endurance exercise performance in Masters athletes: age-associated changes and underlying physiological mechanisms. J. Physiol. *586*, 55–63. https://doi.org/10.1113/jphysiol.2007.141879.

66. Nanami, A. (2007). Juvenile swimming performance of three fish species on an exposed sandy beach in Japan. J. Exp. Mar. Biol. Ecol. *348*, 1–10. https://doi.org/10.1016/j.jembe.2007.02.016.

67. Pettersson, L.B., and Brönmark, C. (1999). Energetic consequences of an inducible morphological defence in crucian carp. Oecologia *121*, 12–18. https://doi.org/10.1007/s004420050901.

68. Schakmann, M., and Korsmeyer, K.E. (2023). Fish swimming mode and body morphology affect the energetics of swimming in a wave-surge water flow. J. Exp. Biol. *226*, jeb244739. https://doi.org/10.1242/jeb.244739.

69. Roux, N., Salis, P., Lee, S.-H., Besseau, L., and Laudet, V. (2020). Anemonefish, a model for Eco-Evo-Devo. EvoDevo *11*, 20. https://doi.org/10.1186/s13227-020-00166-7.

70. Klann, M., Mercader, M., Salis, P., Reynaud, M., Roux, N., Laudet, V., and Besseau, L. (2021). Anemonefishes. In Handbook of Marine Model Organisms in Experimental Biology (CRC Press), pp. 443–464. https://doi.org/10.1201/9781003217503-24.

71. Frédérich, B., Fabri, G., Lepoint, G., Vandewalle, P., and Parmentier, E. (2009). Trophic niches of thirteen damselfishes (Pomacentridae) at the Grand Récif of Toliara, Madagascar. Ichthyol. Res. *56*, 10–17. https://doi.org/10.1007/s10228-008-0053-2.

72. Frédérich, B., Olivier, D., Litsios, G., Alfaro, M.E., and Parmentier, E. (2014). Trait decoupling promotes evolutionary diversification of the trophic and acoustic system of damselfishes. Proc. Biol. Sci. *281*, 20141047. https://doi.org/10.1098/rspb.2014.1047.

73. Metcalfe, N.B., Van Leeuwen, T.E., and Killen, S.S. (2016). Does individual variation in metabolic phenotype predict fish behaviour and performance? J. Fish Biol. *88*, 298–321. https://doi.org/10.1111/jfb.12699.

74. Killen, S.S., Nadler, L.E., Grazioso, K., Cox, A., and McCormick, M.I. (2021). The effect of metabolic phenotype on sociability and social group size preference in a coral reef fish. Ecol. Evol. *11*, 8585–8594. https://doi.org/10.1002/ece3.7672.

75. Schmiege, P.F.P., D'Aloia, C.C., and Buston, P.M. (2017). Anemonefish personalities influence the strength of mutualistic interactions with host sea anemones. Mar. Biol. *164*, 24. https://doi.org/10.1007/s00227-016-3053-1.

76. Cleveland, A., Verde, E.A., and Lee, R.W. (2011). Nutritional exchange in a tropical tripartite symbiosis: direct evidence for the transfer of nutrients from anemonefish to host anemone and zooxanthellae. Mar. Biol. *158*, 589–602. https://doi.org/10.1007/s00227-010-1583-5.

77. Hayashi, K., Tachihara, K., Reimer, J.D., and Laudet, V. (2022). Colour patterns influence symbiosis and competition in the anemonefish–host anemone symbiosis system. Proc. Biol. Sci. *289*, 20221576. https://doi.org/10.1098/rspb.2022.1576.

78. Camp, E.F., Hobbs, J.-P.A., De Brauwer, M., Dumbrell, A.J., and Smith, D.J. (2016). Cohabitation promotes high diversity of clownfishes in the Coral Triangle. Proc. Biol. Sci. *283*, 20160277. https://doi.org/10.1098/rspb.2016.0277.

79. Hattori, A. (2002). Small and large anemonefishes can coexist using the same patchy resources on a coral reef, before habitat destruction. J. Anim. Ecol. *71*, 824–831. https://doi.org/10.1046/j.1365-2656.2002.00649.x.

80. Edwards, R.A., and Smith, S.D.A. (2005). Subtidal assemblages associated with a geotextile reef in south-east Queensland, Australia. Mar. Freshw. Res. *56*, 133. https://doi.org/10.1071/MF04202.

81. Hubbell, S.P. (2006). Neutral theory and evolution of ecological equivalence. Ecology *87*, 1387–1398. https://doi.org/10.1890/0012-9658(2006)87[1387:NTATEO]2.0.CO;2.

82. Palmer, T.M., Stanton, M.L., and Young, T.P. (2003). Competition and coexistence: exploring mechanisms that restrict and maintain diversity within mutualist guilds. Am. Nat. *162*, S63–S79. https://doi.org/10.1086/378682.

83. Gainsford, A., van Herwerden, L., and Jones, G.P. (2015). Hierarchical behaviour, habitat use and species size differences shape evolutionary outcomes of hybridization in a coral reef fish. J. Evol. Biol. *28*, 205–222. https://doi.org/10.1111/jeb.12557.

84. Litsios, G., and Salamin, N. (2014). Hybridisation and diversification in the adaptive radiation of clownfishes. BMC Evol. Biol. *14*, 245. https://doi.org/10.1186/s12862-014-0245-5.

85. Gainsford, A., Jones, G.P., Hobbs, J.A., Heindler, F.M., and van Herwerden, L. (2020). Species integrity, introgression, and genetic variation across a coral reef fish hybrid zone. Ecol. Evol. *10*, 11998–12014. https://doi.org/10.1002/ece3.6769.

86. Gaboriau, T., Marcionetti, A., Garcia-Jimenez, A., Schmid, S., Fitzgerald, L.M., Micheli, B., Titus, B., and Salamin, N. (2025). Host use drives convergent evolution in clownfish. Proc. Natl. Acad. Sci. USA *122*, e2419716122. https://doi.org/10.1073/pnas.2419716122.

87. Todd Streelman, J.T., and Danley, P.D. (2003). The stages of vertebrate evolutionary radiation. Trends Ecol. Evol. *18*, 126–131. https://doi.org/10.1016/S0169-5347(02)00036-8.

88. Danley, P.D., and Kocher, T.D. (2001). Speciation in rapidly diverging systems: lessons from Lake Malawi. Mol. Ecol. *10*, 1075–1086. https://doi.org/10.1046/j.1365-294x.2001.01283.x.

89. Muschick, M., Indermaur, A., and Salzburger, W. (2012). Convergent evolution within an adaptive radiation of cichlid fishes. Curr. Biol. *22*, 2362–2368. https://doi.org/10.1016/j.cub.2012.10.048.

90. Losos, J.B. (2011). Convergence, adaptation, and constraint. Evolution *65*, 1827–1840. https://doi.org/10.1111/j.1558-5646.2011.01289.x.

91. Duran-Nebreda, S., Vidiella, B., Spiridonov, A., Eldredge, N., O'Brien, M.J., Bentley, R.A., and Valverde, S. (2024). The many ways toward punctuated evolution. Palaeontology *67*, e12731. https://doi.org/10.1111/pala.12731.

92. Grossnickle, D.M., Brightly, W.H., Weaver, L.N., Stanchak, K.E., Roston, R.A., Pevsner, S.K., Stayton, C.T., Polly, P.D., and Law, C.J. (2024). Challenges and advances in measuring phenotypic convergence. Evolution *78*, 1355–1371. https://doi.org/10.1093/evolut/qpae081.

93. Foote, M. (1997). The evolution of morphological diversity. Annu. Rev. Ecol. Syst. *28*, 129–152. https://doi.org/10.1146/annurev.ecolsys.28.1.129.

94. Frédérich, B., Sorenson, L., Santini, F., Slater, G.J., and Alfaro, M.E. (2013). Iterative ecological radiation and convergence during the evolutionary history of damselfishes (Pomacentridae). Am. Nat. *181*, 94–113. https://doi.org/10.1086/668599.

95. Marcionetti, A., Rossier, V., Roux, N., Salis, P., Laudet, V., and Salamin, N. (2019). Insights into the genomics of clownfish adaptive radiation: genetic basis of the mutualism with sea anemones. Genome Biol. Evol. *11*, 869–882. https://doi.org/10.1093/gbe/evz042.

96. Donelson, J.M., Romans, P., Yamanaka, S., Kinoshita, M., and Roux, N. (2022). Anemonefish husbandry. In Evolution, Development and Ecology of Anemonefishes (CRC Press), pp. 237–252. https://doi.org/10.1201/9781003125365-27.

97. Nanninga, G.B., Côté, I.M., Beldade, R., and Mills, S.C. (2017). Behavioural acclimation to cameras and observers in coral reef fishes. Ethology *123*, 705–711. https://doi.org/10.1111/eth.12642.

98. Tudorache, C., Viaene, P., Blust, R., Vereecken, H., and De Boeck, G. (2008). A comparison of swimming capacity and energy use in seven European freshwater fish species. Ecol. Freshw. Fish *17*, 284–291. https://doi.org/10.1111/j.1600-0633.2007.00280.x.

99. Christopher, J.F. (2010). The role of swimming in reef fish ecology. In Fish Locomotion, P. Domenici, and B.G. Kapoor, eds. (CRC Press), pp. 374–406. https://doi.org/10.1201/b10190-12.

100. Garland, T., and Arnold, S.J. (1983). Effects of a full stomach on locomotory performance of juvenile garter snakes (Thamnophis elegans). Copeia *1983*, 1092. https://doi.org/10.2307/1445117.

101. Huang, W.-X., Shin, S.J., and Sung, H.J. (2007). Simulation of flexible filaments in a uniform flow by the immersed boundary method. J. Comp. Phys. *226*, 2206–2228. https://doi.org/10.1016/j.jcp.2007.07.002.

102. Rosti, M.E., Cavaiola, M., Olivieri, S., Seminara, A., and Mazzino, A. (2021). Turbulence role in the fate of virus-containing droplets in violent expiratory events. Phys. Rev. Research *3*, 013091. https://doi.org/10.1103/PhysRevResearch.3.013091.

103. Rosti, M.E., Olivieri, S., Cavaiola, M., Seminara, A., and Mazzino, A. (2020). Fluid dynamics of COVID-19 airborne infection suggests urgent data for a scientific design of social distancing. Sci. Rep. *10*, 22426. https://doi.org/10.1038/s41598-020-80078-7.

104. Cavaiola, M., Olivieri, S., Guerrero, J., Mazzino, A., and Rosti, M.E. (2022). Role of barriers in the airborne spread of virus-containing droplets: A study based on high-resolution direct numerical simulations. Phys. Fluids *34*, 015104. https://doi.org/10.1063/5.0072840.

105. Sagong, W., Jeon, W.-P., and Choi, H. (2013). Hydrodynamic characteristics of the sailfish (Istiophorus platypterus) and swordfish (Xiphias gladius) in gliding postures at their cruise speeds. PLoS One *8*, e81323. https://doi.org/10.1371/journal.pone.0081323.

106. Ayachit, U. (2015). The ParaView Guide: A Parallel Visualization Application (Kitware, Inc.).

107. Gans, C. (1982). Fiber architecture and muscle function. Exer. Sport Sci. Rev. *10*, 160–207. https://doi.org/10.1249/00003677-198201000-00006.

108. Powell, P.L., Roy, R.R., Kanim, P., Bello, M.A., and Edgerton, V.R. (1984). Predictability of skeletal muscle tension from architectural determinations in guinea pig hindlimbs. J. Appl. Physiol. Respir. Environ. Exerc. Physiol. *57*, 1715–1721. https://doi.org/10.1152/jappl.1984.57.6.1715.

109. Dick, T.J.M., and Clemente, C.J. (2017). Where have all the giants gone? How animals deal with the problem of size. PLoS Biol. *15*, e2000473. https://doi.org/10.1371/journal.pbio.2000473.

110. Allen, V., Elsey, R.M., Jones, N., Wright, J., and Hutchinson, J.R. (2010). Functional specialization and ontogenetic scaling of limb anatomy in *Alligator mississippiensis*. J. Anat. *216*, 423–445. https://doi.org/10.1111/j.1469-7580.2009.01202.x.

111. Allen, V., Molnar, J., Parker, W., Pollard, A., Nolan, G., and Hutchinson, J.R. (2014). Comparative architectural properties of limb muscles in C rocodylidae and A lligatoridae and their relevance to divergent use of asymmetrical gaits in extant C rocodylia. J. Anat. *225*, 569–582. https://doi.org/10.1111/joa.12245.

112. Martin, M.L., Travouillon, K.J., Fleming, P.A., and Warburton, N.M. (2020). Review of the methods used for calculating physiological cross-sectional area (PCSA) for ecological questions. J. Morphol. *281*, 778–789. https://doi.org/10.1002/jmor.21139.

113. R Core Team (2022). R: A Language and Environment for Statistical Computing (R Foundation for Statistical Computing).

114. Martino, C., Morton, J.T., Marotz, C.A., Thompson, L.R., Tripathi, A., Knight, R., and Zengler, K. (2019). A novel sparse compositional technique reveals microbial perturbations. mSystems *4*, e00016–e00019. https://doi.org/10.1128/mSystems.00016-19.

115. Okasen, J., Blanchet, G., Friendly, M., Kindt, R., Legendre, P., McGlinn, D., Minchin, P., O'Hara, R., Simpson, G., Solymos, P., et al. (2022). vegan: Community Ecology Package. R package version 2.6-2. http://CRAN.Rproject.org/package=vegan.

116. Wickham, H. (2016). ggplot2: Elegant Graphics for Data Analysis (Springer).

117. Dinno, A. (2017). dunn.test: Dunn's Test of Multiple Comparisons Using Rank Sums. R package version 1.3.5. https://cran.r-project.org/web/packages/dunn.test/dunn.test.pdf.

118. Leys, C., Ley, C., Klein, O., Bernard, P., and Licata, L. (2013). Detecting outliers: Do not use standard deviation around the mean, use absolute deviation around the median. J. Exp. Soc. Psychol. *49*, 764–766. https://doi.org/10.1016/j.jesp.2013.03.013.

119. Revell, L.J. (2012). phytools: an R package for phylogenetic comparative biology (and other things). Methods Ecol. Evol. *3*, 217–223. https://doi.org/10.1111/j.2041-210X.2011.00169.x.

120. Revell, L.J. (2013). Two new graphical methods for mapping trait evolution on phylogenies. Methods Ecol. Evol. *4*, 754–759. https://doi.org/10.1111/2041-210X.12066.

121. Felsenstein, J. (1985). Phylogenies and the comparative method. Am. Nat. *125*, 1–15. https://doi.org/10.1086/284325.

122. Clavel, J., Escarguel, G., and Merceron, G. (2015). mv morph: An r package for fitting multivariate evolutionary models to morphometric data. Methods Ecol. Evol. *6*, 1311–1319. https://doi.org/10.1111/2041-210X.12420.

STAR★METHODS

KEY RESOURCES TABLE

REAGENT or RESOURCE	SOURCE	IDENTIFIER
Deposited data		
Micro-CTscans of whole anemonefish (6 species)	This paper	https://doi.org/10.5061/dryad.70rxwdc73
Software and algorithms		
Codes for computational simulation of water flow	This paper	https://www.oist.jp/research/research-units/cffu/fujin
Amira (version 6.5.0)	Thermo Fisher Scientific, Waltham, Massachusetts, USA	N/A
Adobe Illustrator	Adobe Inc., 2019	https://adobe.com/products/illustrator
R (version 4.2.1)	R core Team	https://www.r-project.org/

EXPERIMENTAL MODEL AND STUDY PARTICIPANT DESIGN

Experiments were performed with the approval of the Okinawa Institute of Science and Technology (OIST) Animal Care and Use Committee (approval number 2020-317). Sixty adult anemonefishes were collected around Okinawa Island (five breeding pairs for each of the six species found in Okinawa (*Amphiprion clarkii*, *A. frenatus*, *A. ocellaris*, *A. perideraion*, *A. polymnus*, and *A. sandaracinos*)). The sex and size of each individual are reported in Table S1. Fish were kept in pairs (a female and a male forming a breeding couple) in plastic tanks of 250 L for the bigger species (*A. clarkii*, *A. frenatus* and *A. polymnus*) and 150 L for the smaller species (*A. ocellaris*, *A. perideraion* and *A. sandaracinos*). The tanks were set outside as part of an open system where fresh marine water flows continuously (temperature is thus that of the ocean, between 20 °C and 25 °C at the time of the experiments). Each tank contained an air stone for extra aeration and a terracotta pot as habitat. Fish were fed twice daily with a homemade mixture (see Roux et al.[69] and Donelson et al.[96] for more information on anemonefish husbandry).

Fish used for micro-CT scanning (three individual of each of the six okinawan species and one indivual for the other 8 species) were either collected by fishermen in Okinawa Island (*A. clarkii*, *A. frenatus*, *A. perideraion*, *A. polymnus*), cultured at OIST Marine Science Station (*A. ocellaris*, and *A. sandaracinos*), or provided by collaborators from Academia Sinica (Taiwan) (*A. percula* and *A. biaculeatus*), CRIOBE (Moorea, French Polynesia) (*A. chrysopterus*), University of Queensland (Australia) (*A. akyndinos*), King Abdullah University of Science and Technology (Saudi Arabia) (*A. bincinctus*) and Okinawa Churashima Foundation (fish collection) (*A. melanopus*, and *A. ephippium*). *A. nigripes* was purchased from an aquarist company. For practical reasons related to size (the specimen must fit in a 50 ml Falcon tube), all μCT scans were performed on juvenile fish, except for one small adult specimen of *A. nigripes*. By juvenile, we mean fish that were not sexually mature but already displayed adult coloration and body shape. Given this size constraint, the specimens scanned can be considered small for the bigger species (e.g., *A. clarkii*, *A. polymnus*) and within the species ranges for smaller species (e.g., *A. ocellaris*, *A. sandaracinos*) (see Data S1 for fish size).

METHOD DETAILS

In situ characterization of host dependence

Five colonies of each of the six anemonefish species inhabiting Okinawan waters (*Amphiprion clarkii*, *A. frenatus*, *A. ocellaris*, *A. perideraion*, *A. polymnus*, and *A. sandaracinos*) were recorded *in situ* to assess their host dependency (details for each colony are given in Figure S2). A diver placed a camera (GoPro 7 or 8 Black edition) in front of the host anemone at a distance sufficient to see the whole anemone and at least 50 cm around it. Each recording session was at least 20 min long. The first 10 minutes were not analyzed as anemonefish need an acclimation time of two to seven minutes after human presence to resume their natural behavior.[97] The following 10 min were divided into 300 pictures (i.e., a snapshot every 2 s) using the VideoProc Converter software. For each image, the female and male position (inside or outside the host anemone) was determined. As only one camera was used, it was impossible to quantitively estimate the distance between the fish and its host when the fish would venture outside the anemone (due to the camera's depth of field). We instead categorized their relative distance to the anemone into three qualitative groups: close (less than 1 BL), medium (between 1 and 2 BL), and far (more than 2 BL up to out of the field of view of the camera). When a fish could not be seen in a picture, its position on the previous and following frames was assessed. If the positions were the same, it was used for the given picture. If not, it was encoded as NA. The resulting data were a proportion of frames for each of the distance categories for each individual. Summarizing the data at the individual level ensures repeated observations are aggregated approximately and treated as independent data points in the following statistical analysis, preventing pseudoreplication.

Critical swimming speed and respirometry

Critical swimming speed (U_{crit}), which is a standard measurement of fish swimming capacities,[37,45,98,99] as well as a suite of metabolic parameters, were determined from measurements of oxygen consumption and water velocity in a swimming tunnel respirometer (Loligo Systems 5L Swim Tunnel and the associated Loligo Systems AutoResp software) on ten individuals (five males, five females) of each of the six anemonefish species present in Okinawa Island (except for *A. polymnus* for which only eight individuals were tested as one died and one got sick before the experiment could be performed).

Prior to the experiments, all fish were anesthetized in 200mg L^{-1} MS222 solution, and the following morphological measurements were taken: weight (in g, ± 0.01), standard length (SL in cm ± 0.1), height and width (measured at the level of the pectoral fin in cm ± 0.1) and body ratio (BR) calculated as $BR = \frac{SL}{height}$. These measurements were implemented in the software to correct for potential blocking effect and can be found in Table S1.

Fish were starved for 24 hours before the experimental trial to ensure that digestion did not affect performance.[100] U_{crit} tests were done at a water temperature of 25°C (± 0.5) and salinity of 35 (± 1). Prior to each experiment, the oxygen probe was calibrated to 100% air saturation in fully aerated seawater and to 0% using N_2 aerated water. Water velocity was calibrated using the Loligo System vane wheel flow probe and flow meter. Fish were placed in the tunnel and acclimatized for 30 min at a flow speed of 1 Body Length (BL) s^{-1} to allow recovery from handling. Flow velocity was then increased in 1 BL s^{-1} increments every 10 min until the fish became fatigued (swept against the downstream mesh and unable to resume swimming within 30 seconds). U_{crit} was calculated for each individual as $U_{crit} = U_i + U_{ii}\frac{t}{\Delta t}$ with U_i the velocity of the penultimate interval (i.e., last velocity interval entirely sustained by the fish), U_{ii} the velocity increment, t elapse time of the last interval before the fish fatigued, Δt the time interval at which velocity was increased.

Mass-specific Oxygen consumption (MO_2 in mgO_2.kg.hr) was automatically measured every 3 min. The Standard Metabolic Rate (SMR, i.e., resting oxygen consumption) was estimated as the mean MO_2 during the first interval (at a velocity of 1 BL), the Maximal Metabolic Rate (MMR, i.e., oxygen consumption during the maximum sustainable rate of exercise) as the highest MO_2 measured during the experiment, the Aerobic scope (A.scope, i.e., the ability to increase oxygen uptake rate) as $A.scope = MMR - SMR$ and the Cost Of Transport (COT) was estimated at U_{crit} as $COT = MO_{2v}/v$ with v the velocity and MO_{2v} the MO2 at v.

Micro-CT scanning

Fish were euthanized in a 400mg / L MS222 solution. They were then fixed in a 10% formalin solution, with fins spread out using insect pins. After a week, the specimens were rinsed in fresh water for an hour and gradually transferred to 70% ethanol as follows: rinsed in fresh water, placed successively in 30% and 50% ethanol baths for three hours, and finally transferred to 70% ethanol for storage. Specimens underwent iodine staining in ethanol before scanning. For detailed staining procedures of fish specimens, see Ziadi-Künzli et al.[53]

All specimens used in this study were deposited in the ichthyological collection of the newly established OIST Natural History Collection at the Okinawa Institute of Science and Technology Graduate University, Okinawa, Japan (OISTICH).

Samples from the museum collection were preserved in 70% ethanol, but the original fixation method is unknown.

Scans were conducted using a Zeiss Xradia Versa 510 (OIST). Scanning of each sample was performed under varying conditions: power settings ranged from 40-100kv, with exposure times between 1-5 seconds. A total of 1601 projections were captured on an Andor camera with an image size of 1004 x 1024. The resulting voxel resolution achieved with a 0.4x objective spanned from 12.8 to 39.7μm.

Computational fluid dynamics simulations

From the μCT-scan data, it was possible to acquire the external surface of one specimen of each of the 14 specimens, which served as the input geometry for computational fluid dynamics (CFD) simulations aimed at characterizing the most relevant hydrodynamical features (i.e., drag force/coefficient and qualitative flow patterns). The numerical simulations have been performed using the in-house code *Fujin* (https://www.oist.jp/research/research-units/cffu/fujin), which combines a finite-difference discretization and fractional step method to solve the incompressible Navier-Stokes equations for the fluid flow, together with an immersed boundary method to model the presence of solid boundaries.[101] The code has been validated for a variety of problems; see Rosti et al.,[102] Rosti et al.,[103] and Cavaiola et al.[104] for example. Specifically, we considered the fish in a fixed and straight configuration, being representative of a steady swimming regime at a constant cruise speed (i.e., in the absence of maneuvers).[105] For the sake of mutual comparison, for all species, we consider the same Reynolds number (based on the fish length, incoming flow velocity, and water viscosity) of 1000, although other values of this nondimensional parameter have also been explored yet giving the same qualitative outcomes. The acquired geometry for each species was discretized onto a triangulated mesh and immersed in a computational box of size 5L x 2L x 2L (with L the total fish length) discretized with 1000 x 400 x 400 nodes in the streamwise, vertical, and spanwise directions, respectively. A uniform velocity profile is imposed at the inlet and a convective boundary condition is prescribed at the outlet, slip conditions apply at the top and bottom boundaries (i.e., normal to the vertical direction), whereas periodic boundary conditions apply along the spanwise direction. The convergence of the numerical results has been verified both against the grid resolution, timestep, and domain size.

Segmentation and visualization of fin and axial muscles

The μCT reconstructions obtained were exported in.txm format and imported into Amira (version 6.5.0, Thermo Fisher Scientific, Waltham, Massachusetts, USA) for the manual segmentation of pectoral fin muscles and axial musculature. This process also involved rendering isosurfaces from the volumetric data to ascertain body volume.

Global thresholding was applied within a gray-scale range of 14,000 to 30,000. Structures were manually annotated using the brush or magic wand tools on every fourth slice and then interpolated for continuity. For the axial musculature specifically, the soft tissue on the left side of the fish was segmented, and the volume was doubled to account for the entire body, excluding the fins, head, gills, and intestinal parts.

A surface generation algorithm, implemented in the *Generate Surface* module, was applied to each material, utilizing smoothing function values < 2.5. The resulting 3D surface meshes were exported in.ply format and imported into the ParaView package for data visualization.[106] Anatomical illustrations were created with Adobe Illustrator (Adobe Inc., 2019., available at: {https://adobe.com/products/illustrator)}.

Physiological cross-sectional area (PCSA)

Skeletal muscle architecture is characterized by the geometric properties of a muscle, including the arrangement of its fibers, which functionally determines muscle performance capacity.[107,108] Key muscle properties such as fiber length (L_f) and physiological cross-sectional area (PCSA) are critical parameters of muscle architecture that influence function. Fiber length is indicative of the muscle's excursion or 'working range,' while PCSA correlates directly with a muscle's force-generating capacity. PCSA of a given muscle can be calculated from the muscle volume (V_m) divided by the mean muscle fiber length (PCSA = V_m/ L_f). To determine the fiber length, we imported each muscle's surface mesh into Checkpoint software (version 2022.12.16, Stratovan Checkpoint, Davis, USA). We repeatedly placed curve points along the structure, from the origin to the insertion of the muscle, repeating this process 5–10 times. We then calculated the mean fiber length for each muscle, which was utilized for subsequent analyses.

Applying geometric similarity principles to length, area, and volume,[109] we normalized muscle fiber length to $V_{body}^{1/3}$, PCSA to $V_{body}^{2/3}$, and muscle volume to V_{body}.[110] This normalization against fish body volume (V_{body}) enables comparison between specimens of varying sizes, facilitating an exploration of the trade-offs between force generation (PCSA) and working range capacities.[109–112] In this study, we compared muscle force production in the pectoral fin across 14 species of anemonefish, as well as the twinspot damselfish (*Chrysiptera biocellata*).

Normalized PCSA values were plotted against mean normalized fiber lengths to generate a functional performance space for pectoral fin muscles of anemone and damselfish. The plot was divided into four quadrants by lines bisecting each axis at their midpoints due to the scaling, which set a maximum of 600 for normalized fiber length and 1.0 for PCSA, enabling comprehensive cross-species comparisons.

This plotting illustrates the relative forces and excursions of muscles, giving an estimation of relative muscle function based on their position in the biplot.[110] The outermost muscles were connected by line segments to create a polygon. From the resulting polygon of each function space plot, we measured the area confined to the upper right quadrant (''powerful'' muscles) by applying an Illustrator area script in Adobe Illustrator that calculates the area of a shape.

Evolution of morphological disparity

After revealing swimming eco-morphotypes in anemonefish from Okinawa Islands, we aimed to explore the evolution of these morphologies across a larger phylogenetic sample of *Amphiprion* species. To do so, we estimated the drag coefficient and muscle volume from μCT for eight additional species (total of 14 species) distributed across the anemonefish evolutionary tree, presenting various pigmentation patterns and host specificity (Figure S1). We also calculated body ratio from pictures available in our lab, provided by collaborators and by Randall J.E., available on Fishbase (n=3 to 13).

The subsequent phylogenetic analyses were based on the damselfish consensus time-tree published by McCord et al.,[54] which includes all the studied anemonefish species. The topology of this tree is congruent with other recently published phylogenies.[25,86] Although some uncertainties remain at shallow phylogenetic levels, the great majority and mostly the deepest nodes of the monophyletic clade of *Amphiprion* (i.e., the tribe Amphiprionini) are well established. We are thus confident that the phylogenetic uncertainty should not impair our results.

QUANTIFICATION AND STATISTICAL ANALYSIS

All statistical analyses were performed using R (version 4.2.1).[113] The specific tests used for each experiment are detailed below. For all statistical tests, significance was determined at $p < 0.05$. Exact *p-value*s and other relevant test parameters are reported in the text, as well as supplemental information, where applicable.

In situ characterization of host dependence

Data were ordinated using non-metric Multidimensional Scaling (nMDS) with the metaMDS() function on a robust Aitchison distance matrix (which fits their compositional nature and the presence of zeros and ones[114]). The effect of species, sex, and their interaction factor (species*sex) on how fish use space was tested by permutational analysis of variance (PERMANOVA) with the adonis2() function using the same distance and 9999 permutations. Both analyses were performed using the *vegan* package[115] and visual representations using the package *ggplot2*.[116]

Critical swimming speed and respirometry

U_{crit} and metabolic parameters were compared between species using Kruskal-Wallis test, function Kruskal.test(), followed, when relevant, by Dunn pairwise test (function dunn.test() from package *dunn.test*[117]) with Bonferroni correction. We applied Principal Component Analysis (PCA), function prcomp(), on the dataset containing COT, $U_{crit,}$ and morphological parameters for each individual to reveal any underlying structure in the data and identify eventual eco-morphotypes. All analyses were run twice. A first time on the complete dataset (result presented in S3). A second time, after removing outliers identified using a double outlier test, boxplot, function boxblot.stats(), and modified z-score (using the median and median absolute deviation),[118] with values exceeding 2.5 considered outliers. Values identified as outliers with at least one method were removed from the dataset. Results from the second analysis are presented in the main manuscript.

Definition of the eco-morphotypes

We combined data from the host dependency study (mean proportion of time spent inside the anemone per species), the respirometry experiment (mean Ucrit and COT per species), morphological traits (mean SL and body ratio per species, volume of axial muscles and of the main pectoral fin muscles), and the drag coefficient. We again applied PCA with the function prcomp() to explore if a similar grouping as with the previous PCA would be recovered.

Evolution of morphological disparity

We assessed divergences along major axes of morphological variation by mapping PC axes (from the PCA described above) on the phylogenetic tree with the function contMap() from the R-package *phytools* v. 2.1-1.[119,120] In brief, the mapping is accomplished by estimating states at internal nodes using maximum likelihood and by interpolating the states along each edge using equations from.[121] These reconstructions helped to visually assess morphospace occupancy patterns, where each of the two first axes of morphological variation from the PCA were plotted along the phylogeny.

Testing for related evolution between swimming morphologies and host specificity

Host specificity varies between anemonefish, and the physiological adaptations associated with this continuum of specialist-generalist *Amphiprion* species are often hypothesized to be the main axis of ecological speciation during their evolution history.[23,32] To investigate the potential evolutionary correlation between swimming eco-morphotypes and the number of used giant sea anemones by anemonefish, we performed multivariate phylogenetic generalized least squares (PGLS) regression using the mvgls() function in the package *mvMORPH*.[122] This approach enabled us to test the relationships between morphology and habitat use while accounting for the expected covariance of traits among species due to shared ancestry. Along these tests, the morphological data were the response variables, and the number of used sea anemones was the explanatory variable. First, we calculated the fit of three models of evolution: Brownian Motion (BM), Ornstein-Uhlenbeck (OU), and Early Burst (EB). Along this comparative framework, we also included an ordinary least squares (OLS) regression in order to check if a model assuming an absence of covariance of traits among species would outperform the three other models. Then, we compared the likelihood of the model fits with Generalized Information Criterion (GIC) to establish which model provided the best fit. Finally, we tested the null hypothesis of an absence of relationship between swimming morphology and number of used sea anemones by using the function manova.gls(), which performs a Wilks multivariate test on the selected linear model.

Current Biology, Volume *35*

Supplemental Information

Integrative phenotyping reveals new insights into the anemonefish adaptive radiation

Manon Mercader, Fabienne Ziadi-Künzli, Stefano Olivieri, Shinya Komoto, Marco Edoardo Rosti, Bruno Frédérich, and Vincent Laudet

A

Species	Color pattern number of bars	Number of hosts	Number of reproductive adult host	Number of primary reproductive host	Primary reproductive host
A. clarkii	2 or 3	10	7	5	Generalist
A. frenatus	1	1	1	1	*Entacmea spp.*
A. ocellaris	3	3	2	1	*R. magnifica*
A. perideraion	1	4	1	1	*R. magnifica*
A. polymnus	2 or 3	3	2	1	*Stichodactyla spp.*
A. sandaracinos	0	2	1	1	*Stichodactyla spp.*
A. akindynos	2	6	5	3	Generalist
A. biaculeatus	3	1	1	1	*Entacmea spp.*
A. bicinctus	2	6	4	3	Generalist
A. chrysopterus	2	7	5	3	Generalist
A. ephippium	0	2	1	1	*Entacmea spp.*
A. melanopus	1 or 2	3	1	1	*Entacmea spp.*
A. nigripes	1	1	1	1	*R. magnifica*
A. percula	3	3	2	1	*R. magnifica*

B

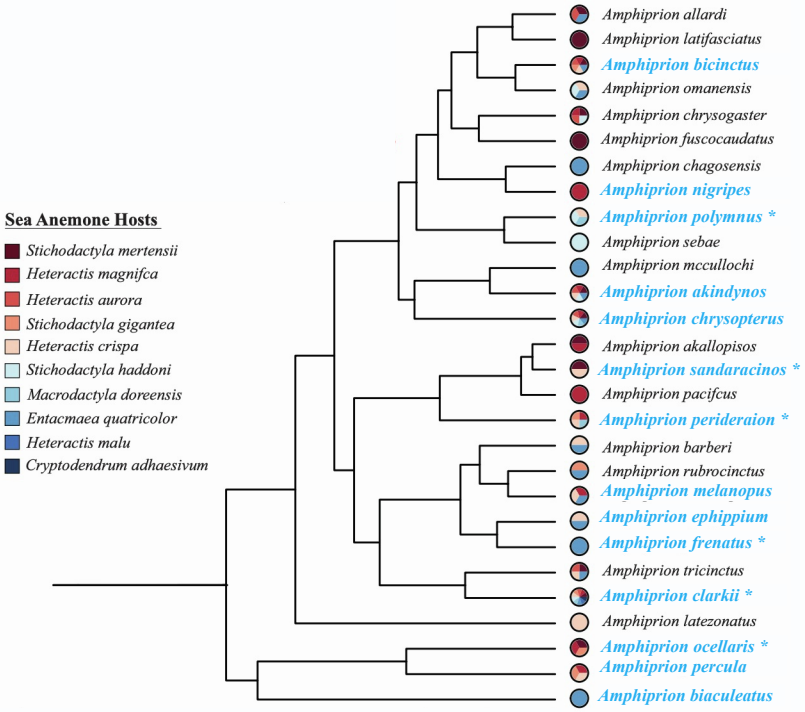

Figure S1: Description of studied species. Related to the STAR method.

A- Description of species color pattern according to Salis et al. 2018[S1], number of hosts according to Fautin & Allen 1997[S2], number of reproductive adult hosts, number and type of primary reproductive host according to Gaboriau et al. 2024[S3]. B- Anemonefishes phylogenetic tree modified from Marcionetti et al. 2022[S4], showing the studied species in blue and those living in Okinawa marked with an *.

A

Fish species	Replicate	Ane. Species	Depth	Group composition
A. clarkii	Colony1	*H. crispa*	5.6	2 sub, 1 *A. perideraion*, cardinalfish
A. clarkii	Colony2	*H. crispa*	5.6	1 sub, cardinalfish
A. clarkii	Colony3	*H. crispa*	6.5	2 sub
A. clarkii	Colony4	*S. mertensii*	5.0	5 sub, 1 *A. sandaracinos*
A. clarkii	Colony5*	*S. mertensii*	15.3	2 *A. sandaracinos*, *D. trimaculatus*, cardinalfish
A. polymnus	Colony1	*S. haddoni*	18.2	3 sub
A. polymnus	Colony2	*S. haddoni*	19.0	2 sub
A. polymnus	Colony3	*S. haddoni*	21.0	5 sub, 1 *A. sandaracinos*
A. polymnus	Colony4	*S. haddoni*	20.0	3 sub
A. polymnus	Colony5	*S. haddoni*	9.3	5 sub
A. frenatus	Colony1	*E. quadricolor*	2.9	1 sub
A. frenatus	Colony2	*E. quadricolor*	2.4	1 sub
A. frenatus	Colony3	*E. quadricolor*	4.8	none
A. frenatus	Colony4	*E. quadricolor*	2.5	1 sub
A. frenatus	Colony5	*E. quadricolor*	8.0	1 sub
A. ocellaris	Colony1	*H. magnifica*	2.1	3 sub
A. ocellaris	Colony2	*H. magnifica*	2.5	1 sub
A. ocellaris	Colony3	*H. magnifica*	6.0	1 sub
A. ocellaris	Colony4	*H. magnifica*	14.0	1 sub
A. ocellaris	Colony5	*H. magnifica*	12.9	1 sub
A. perideraion	Colony1	*H. crispa*	4.5	none
A. perideraion	Colony2	*H. crispa*	13.0	none
A. perideraion	Colony3	*H. crispa*	9.5	none
A. perideraion	Colony4	*H. crispa*	14.7	none
A. perideraion	Colony5	*H. crispa*	16.0	none
A. sandaracinos	Colony1	*S. mertensii*	3.2	2 sub
A. sandaracinos	Colony2	*S. mertensii*	2.3	1 sub
A. sandaracinos	Colony3	*S. mertensii*	4.1	1 sub
A. sandaracinos	Colony4*	*S. mertensii*	15.3	2 *A. clarkii*, *D. trimaculatus*, cardinalfish
A. sandaracinos	Colony5	*S. mertensii*	7.2	2 *A. clarkii, D. trimaculatus*

* This was the same anemone

B

Factors	Df	Sum Sq	R^2	Pseudo-F	P
Species	5	97.555	0.3627	5.9779	**0.0001**
Sex	1	2.781	0.0103	0.8520	0.4551
Species * Sex	5	11.962	0.0445	0.7330	0.7296
Residual	48	156.665	0.5825		
Total	59	268.920	1.0000		

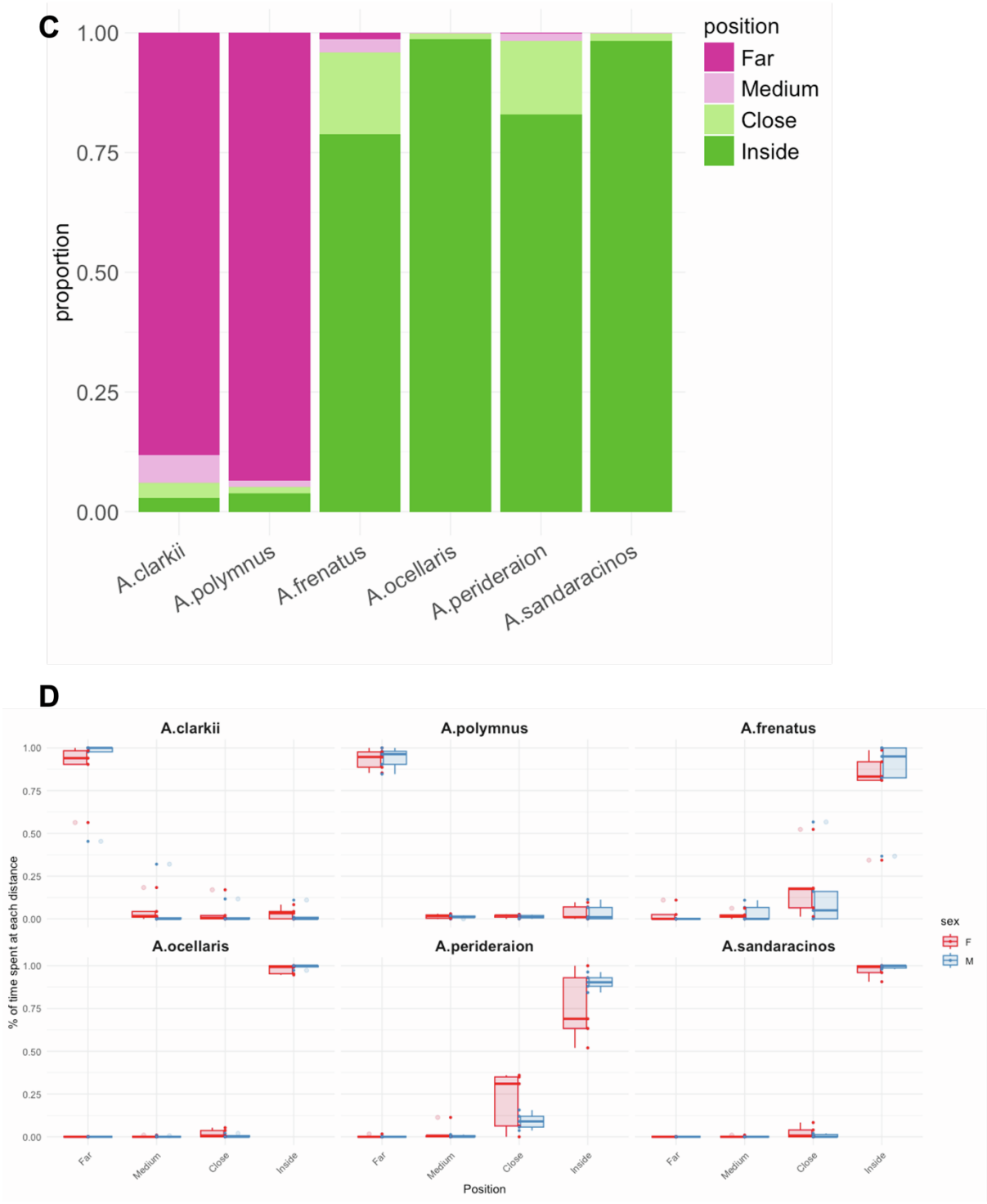

Figure S2: Supporting information for *in situ* video recordings. Related to Figure 1.
A- Characteristics of the recorded colonies. Sub=subadults, including new recruits. B- PERMANOVA results table. C- Stacked histogram representing average host use (proportion of time spent in each area over a 10-minute period) for each species. D- Boxplot of the proportion of time spent in each area for females and males of each species showing the first and third quartile (bottom and top of the box) median (middle horizontal bar) and minimal and maximal values (whiskers).

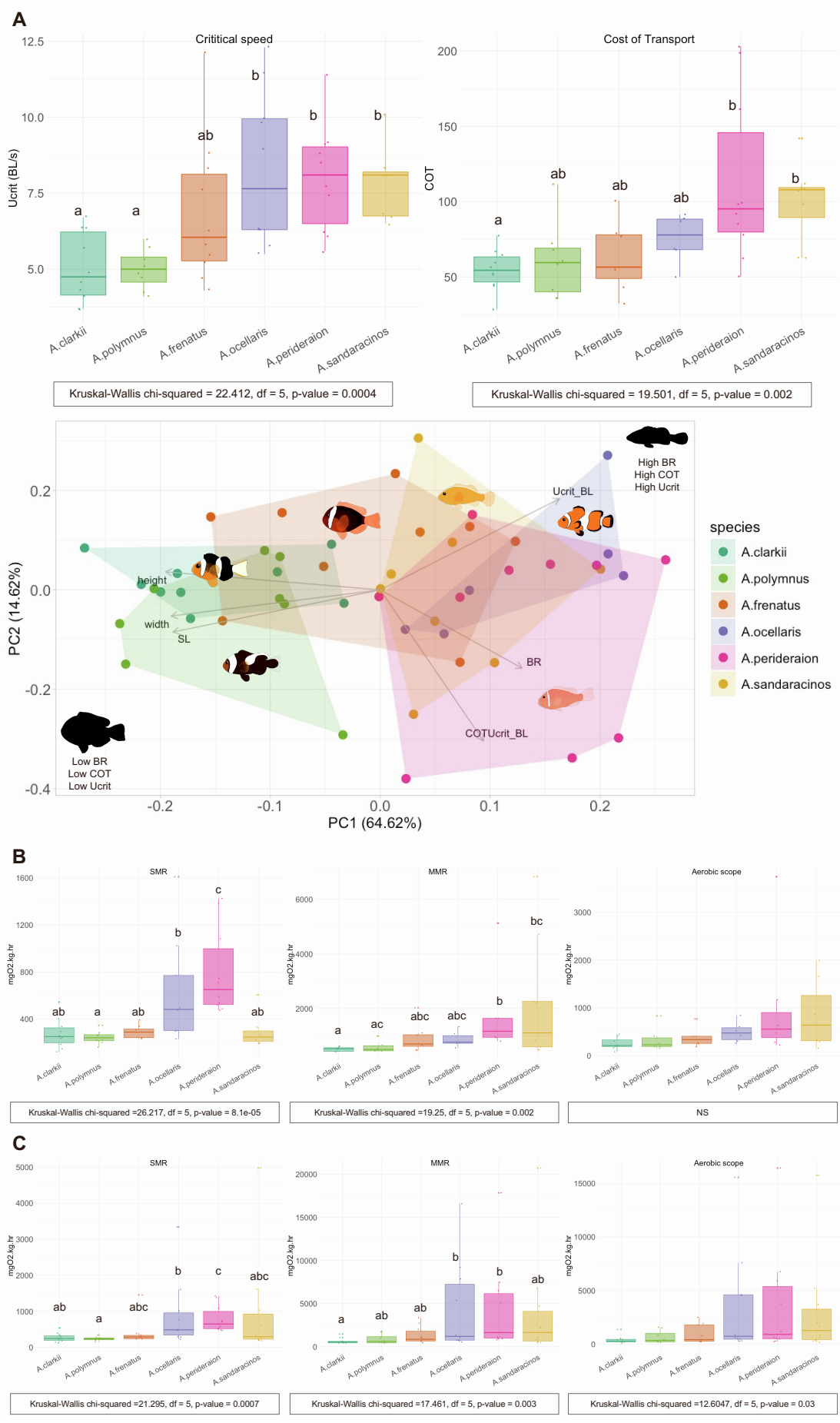
A
Critical speed
Ucrit (BL/s)
12.5
10.0
7.5
5.0
a
a
ab
b
b
b
A.clarkii
A.polymnus
A.frenatus
A.ocellaris
A.perideraion
A.sandaracinos
Kruskal-Wallis chi-squared = 22.412, df = 5, p-value = 0.0004
Cost of Transport
COT
200
150
100
50
a
ab
ab
ab
b
b
Kruskal-Wallis chi-squared = 19.501, df = 5, p-value = 0.002
High BR
High COT
High Ucrit
Low BR
Low COT
Low Ucrit
Ucrit_BL
height
width
SL
BR
COTUcrit_BL
PC2 (14.62%)
PC1 (64.62%)
0.2
0.0
-0.2
-0.4
-0.2
-0.1
0.0
0.1
0.2
species
A.clarkii
A.polymnus
A.frenatus
A.ocellaris
A.perideraion
A.sandaracinos
B
SMR
MMR
Aerobic scope
mgO2.kg.hr
Kruskal-Wallis chi-squared =26.217, df = 5, p-value = 8.1e-05
Kruskal-Wallis chi-squared =19.25, df = 5, p-value = 0.002
NS
C
SMR
MMR
Aerobic scope
mgO2.kg.hr
Kruskal-Wallis chi-squared =21.295, df = 5, p-value = 0.0007
Kruskal-Wallis chi-squared =17.461, df = 5, p-value = 0.003
Kruskal-Wallis chi-squared =12.6047, df = 5, p-value = 0.03

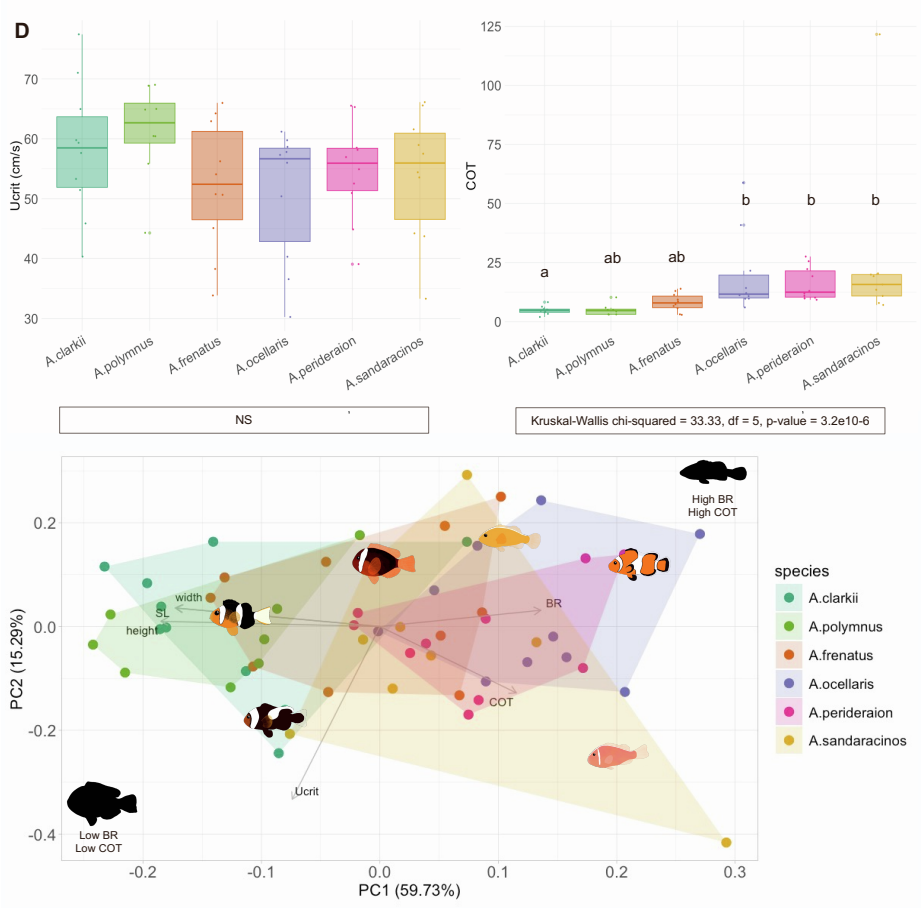
D
Ucrit (cm/s)
COT
A.clarkii
A.polymnus
A.frenatus
A.ocellaris
A.perideraion
A.sandaracinos
a
ab
ab
b
b
b
NS
Kruskal-Wallis chi-squared = 33.33, df = 5, p-value = 3.2e10-6
PC2 (15.29%)
PC1 (59.73%)
width
SL
height
BR
COT
Ucrit
High BR
High COT
Low BR
Low COT
species
A.clarkii
A.polymnus
A.frenatus
A.ocellaris
A.perideraion
A.sandaracinos

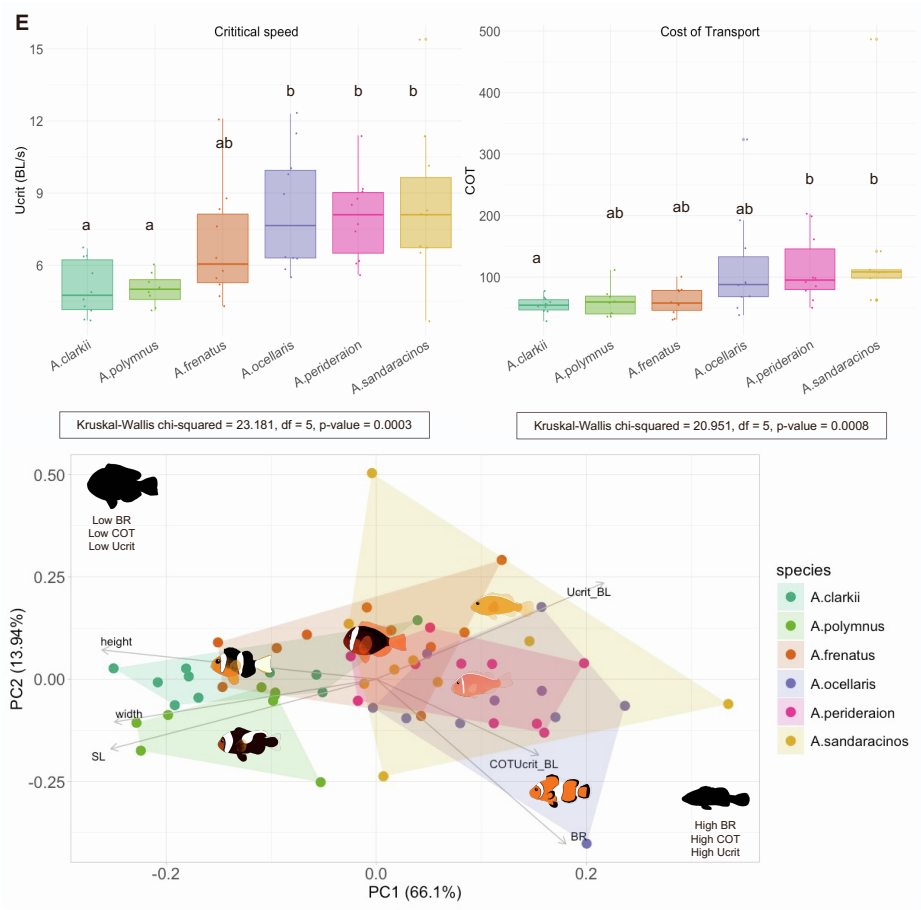
E
Critical speed
Cost of Transport
Ucrit (BL/s)
COT
A.clarkii
A.polymnus
A.frenatus
A.ocellaris
A.perideraion
A.sandaracinos
a
a
ab
b
b
b
a
ab
ab
ab
b
b
Kruskal-Wallis chi-squared = 23.181, df = 5, p-value = 0.0003
Kruskal-Wallis chi-squared = 20.951, df = 5, p-value = 0.0008
PC2 (13.94%)
PC1 (66.1%)
Low BR
Low COT
Low Ucrit
height
width
SL
Ucrit_BL
COTUcrit_BL
BR
High BR
High COT
High Ucrit
species
A.clarkii
A.polymnus
A.frenatus
A.ocellaris
A.perideraion
A.sandaracinos

F

without ouliers	*A.clarkii*	*A.polymnus*	*A.frenatus*	*A.ocellaris*	*A.perideraion*	*A.sandaracinos*
SL (cm)	9.8 ± 0.2 (9)	10.0 ± 0.4 (8)	6.7 ± 0.5 (10)	5.2 ± 0.4 (10)	5.7 ± 0.3 (10)	5.6 ± 0.4 (10)
height (cm)	4.1 ± 0.3 (10)	3.8 ± 0.2 (8)	2.9 ± 0.3 (10)	1.6 ± 0.2 (10)	2.0 ± 0.2 (10)	2.2 ± 0.3 (10)
width (cm)	1.4 ± 0.2 (10)	1.8 ± 0.2 (8)	0.9 ± 0.1 (10)	0.6 ± 0.1 (10)	0.6 ± 0.1 (10)	0.8 ± 0.1 (10)
weight (cm)	44.4 ± 6.7 (10)	44.2 ± 6.1 (10)	17.3 ± 3.8 (10)	5.9 ± 1.2 (10)	7.7 ± 1.5 (10)	7.3 ± 1.4 (10)
BR	2.3 ± 0.1 (10)	2.7 ± 0.1 (8)	2.4 ± 0.1 (10)	3.4 ± 0.2 (10)	3.0 ± 0.2 (10)	2.8 ± 0.3 (10)
Ucrit (BL/s)	5.1 ± 0.4 (10)	5.0 ± 0.2 (8)	6.9 ± 0.8 (10)	8.3 ± 0.8 (10)	8.0 ± 0.6 (10)	7.7 ± 0.7 (9)
Ucrit (cm/s)	58.1 ± 3.5 (10)	63.5 ± 1.8 (7)	52.2 ± 3.4 (10)	53.1 ± 3.0 (9)	56.4 ± 2.2 (9)	53.9 ± 3.3 (10)
SMR mgO2/kg/h)	274.8 ± 40.0 (10)	242.3 ± 20.2 (8)	288.8 ± 19.7 (8)	630.7 ± 148.3 (9)	794.8 ± 116.6 (10)	292.6 ± 54.9 (7)
MMR (mgO2/kg/h)	515.5 ± 29.6 (8)	592.5 ± 87.7 (6)	898.1 ± 180.0 (8)	872.7 ± 115.6 (6)	1752.9 ± 576.4 (7)	2170.4 ± 738.4 (9)
A.scope (mgO2/kg/h)	254.7 ± 44.1 (8)	342.3 ± 105.0 (6)	383.1 ± 85.4 (6)	493.8 ± 87.3 (6)	1011.8 ± 469.6 (7)	848.3 ± 270.1 (7)
COT(BL)	54.6 ± 4.3 (10)	60.6 ± 8.8 (8)	61.5 ± 8.0 (9)	75.7 ± 6.6 (6)	112.9 ± 17.4 (10)	100.3 ± 9.3 (8)
COT(cm)	4.5 ± 0.4 (9)	4.3 ± 0.4 (7)	7.9 ± 1.3 (9)	11.4 ± 0.7 (6)	16.0 ± 2.2 (10)	14.4 ± 1.9 (8)
complete	*A.clarkii*	*A.polymnus*	*A.frenatus*	*A.ocellaris*	*A.perideraion*	*A.sandaracinos*
SL (cm)	9.3 ± 0.6 (10)	10.0 ± 0.4 (8)	6.7 ± 0.5 (10)	5.2 ± 0.4 (10)	5.7 ± 0.3 (10)	5.6 ± 0.4 (10)
height (cm)	4.1 ± 0.3 (10)	3.8 ± 0.2 (8)	2.9 ± 0.3 (10)	1.6 ± 0.2 (10)	2.0 ± 0.2 (10)	2.2 ± 0.3 (10)
width (cm)	1.4 ± 0.2 (10)	1.8 ± 0.2 (8)	0.9 ± 0.1 (10)	0.6 ± 0.1 (10)	0.6 ± 0.1 (10)	0.8 ± 0.1 (10)
weight (cm)	44.4 ± 6.7 (10)	44.2 ± 6.1 (8)	17.3 ± 3.8 (10)	5.9 ± 1.2 (10)	7.7 ± 1.5 (10)	7.3 ± 1.4 (10)
BR	2.3 ± 0.1 (10)	2.7 ± 0.1 (8)	2.4 ± 0.1 (10)	3.4 ± 0.2 (10)	3.0 ± 0.2 (10)	2.8 ± 0.3 (10)
Ucrit (BL/s)	5.1 ± 0.4 (10)	5.0 ± 0.2 (8)	6.9 ± 0.8 (10)	8.3 ± 0.8 (10)	8.0 ± 0.6 (10)	8.5 ± 1.0 (10)
Ucrit (cm/s)	58.1 ± 3.5 (10)	61.1 ± 2.9 (8)	52.2 ± 3.4 (10)	50.8 ± 3.5 (10)	54.7 ± 2.6 (10)	53.9 ± 3.3 (10)
SMR mgO2/kg/h)	274.8 ± 40.0 (10)	242.3 ± 20.2 (8)	418.5 ± 130.8 (9)	901.8 ± 301.8 (10)	794.8 ± 116.6 (10)	967.4 ± 468.8 (10)
MMR (mgO2/kg/h)	667.0 ± 108.1 (10)	884.1 ± 201.6 (8)	1328.9 ± 323.9 (10)	4428.6 ± 1698.4 (10)	4412.5 ± 1693.3 (10)	4026.1 ± 1969.8 (10)
A.scope (mgO2/kg/h)	392.2 ± 116.1 (10)	641.8 ± 210.7 (8)	944.8 ± 293.1 (9)	3526.8 ± 1560.0 (10)	3617.8 ± 1619.4 (10)	3058.7 ± 1503.7 (10)
COT(BL)	54.6 ± 4.3 (10)	60.6 ± 8.8 (8)	61.3 ± 7.2 (10)	115.6 ± 27.3 (10)	112.9 ± 17.4 (10)	143.2 ± 43.7 (9)
COT(cm)	4.9 ± 0.5 (10)	5.0 ± 0.8 (8)	8.2 ± 1.2 (10)	19.6 ± 5.4 (10)	16.0 ± 2.2 (10)	26.3 ± 12.0 (9)

Figure S3: Supporting information for respirometry experiments. Related to Figure 2.

A- Boxplot and PCA for size-normalized data on the dataset without outliers. Boxplot of Ucrit (in BL/s) and COT showing the first and third quartile (bottom and top of the box), median (middle horizontal bar), and minimal and maximal values (whiskers) for each species. Results of pairwise comparisons are indicated by lower-case letters; species sharing a letter do not differ from each other.

B- Boxplot of Standard Metabolic Rate (SMR), Maximal Metabolic Rate (MMR), and Aerobic scope (A. scope) for each species on the dataset without outliers. Results of pairwise comparisons are indicated by lower-case letters; species sharing a letter do not differ from each other.

C- Boxplot of Standard Metabolic Rate (SMR), Maximal Metabolic Rate (MMR), and Aerobic scope (A. scope) for each species on the complete dataset. Results of pairwise comparisons are indicated by lower-case letters; species sharing a letter do not differ from each other.

D- Boxplot and PCA for absolute data on the complete dataset. Boxplot of Ucrit (in cm/s) and COT showing the first and third quartile (bottom and top of the box), median (middle horizontal bar), and minimal and maximal values (whiskers) for each species. Results of pairwise comparisons are indicated by lower-case letters; species sharing a letter do not differ from each other.

E- Boxplot and PCA for size-normalized data on the complete dataset. Boxplot of Ucrit (in BL/s) and COT showing the first and third quartile (bottom and top of the box), median (middle horizontal bar), and minimal and maximal values (whiskers) for each species. Results of pairwise comparisons are indicated by lower-case letters; species sharing a letter do not differ from each other.

F- Summary table with mean value ± standard error for each species and variable for the dataset without outliers and the complete dataset.

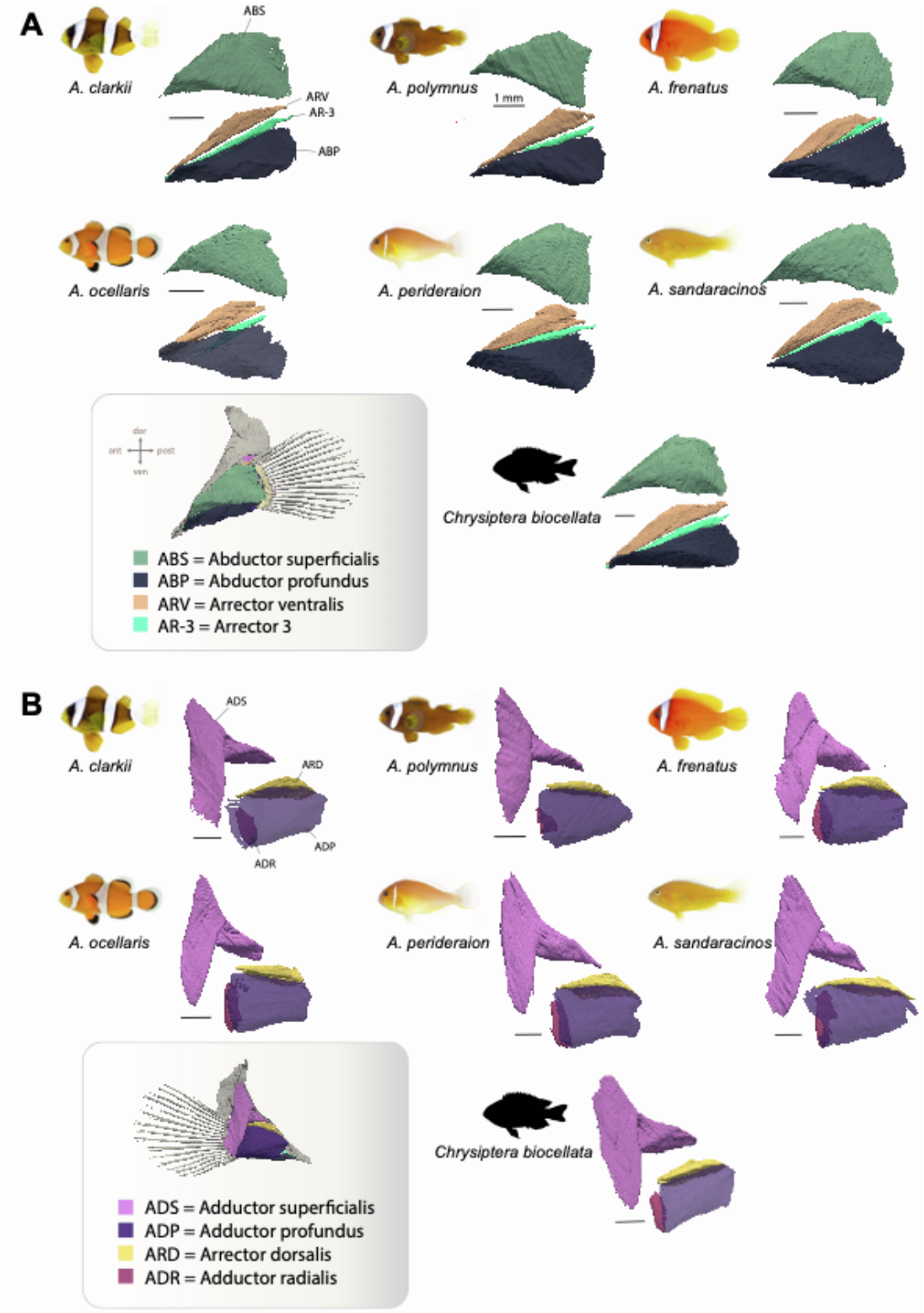

Figure S4: Pectoral fin muscles in the six species of anemonefishes from Okinawa Island. Related to Figure 4. The damselfish *C. biocellata* is added for comparison (note the very similar structure). A- The lateral fin musculature in modern ray-finned fish comprises a superficial and deep abductor (abductor superficialis, abductor profundus) and two arrector muscle (arrector ventralis, arrector 3). B- The medial fin musculature in modern ray-finned fish comprises a superficial and deep adductor (adductor superficialis, adductor profundus), one arrector muscle (arrector dorsalis) and a vestigial adductor on the proximal radials (adductor radialis). Individual fish images are not to scale.

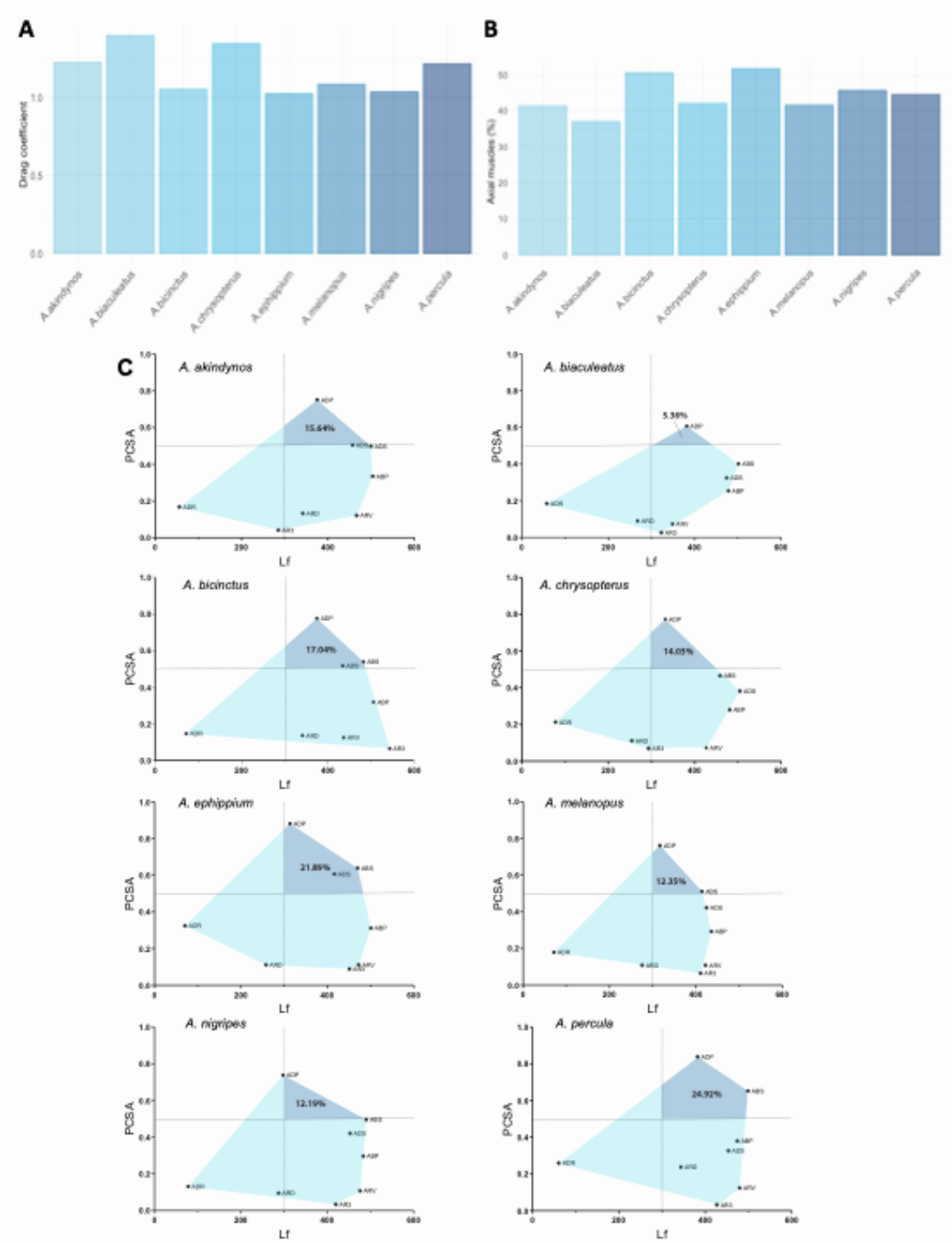

S5 Figure: Supporting information for the additional eight species. Related to Figure 5.
A- Drag coefficient for the eight additional species. B- Drag coefficient for the eight additional species. Both histogram representations are for visual clarity and represent one value for each species. C- Functional space plot of pectoral fin muscles (ABP: abductor profondus, ABS: abductor superficialis, ADP: adductor profondus, ADS: adductor superficialis, ADR: adductor radialis, ARD: arrector dorsalis, ARV: arrector ventralis and AR 3: arrector-3, for the eight additional anemonefish species. The fiber length (Lf, x-axis) reflects a muscle's excursion or 'working range.' It is plotted against the physiological cross-sectional area (PCSA, y-axis), which is directly proportional to the force-generating capacities of a given muscle.

Supplemental References

S1. Salis, P., Lorin, T., Lewis, V., Rey, C., Marcionetti, A., Escande, M., Roux, N., Besseau, L., Salamin, N., Sémon, M., et al. (2019). Developmental and comparative transcriptomic identification of iridophore contribution to white barring in clownfish. Pigment Cell Melanoma Res *32*, 391–402. https://doi.org/10.1111/pcmr.12766.

S2. Fautin, D.G., and Allen, G.R. (1997). Anemone Fishes and Their Host Sea Anemones: A Guide for Aquarists and Divers (Western Australian Museum).

S3. Gaboriau, T., Marcionetti, A., Garcia Jimenez, A., Schmid, S., Fitzgerald, L.M., Micheli, B., Titus, B., and Salamin, N. (2024). Host-use Drives Convergent Evolution in Clownfish and Disentangles the Mystery of an Iconic Adaptive Radiation. Preprint, https://doi.org/10.1101/2024.07.08.602550 https://doi.org/10.1101/2024.07.08.602550.

S4. Marcionetti, A., Schmid, S., and Salamin, N. (2022). Genomic Evidence of Hybridization during the Evolution of Anemonefishes. In Evolution, Development and Ecology of Anemonefishes (CRC Press), pp. 29–40. https://doi.org/10.1201/9781003125365-5.